
Cumulative Glare Analysis Report

March Air Reserve Base

Compatible Use Study

OCTOBER 2023

Prepared for:

COUNTY OF RIVERSIDE
AIRPORT LAND USE COMMISSION
4080 Lemon Street, 14th Floor
Riverside, California 92501

Prepared by:

DUDEK

38 North Marengo Avenue
Pasadena, California 91101

Table of Contents

SECTION	PAGE NO.
Acronyms and Abbreviations.....	iii
1 Introduction.....	1
1.1 Purpose and Scope.....	1
1.2 General Concepts of Solar Technologies and Glare.....	1
2 Source and Receptor Overview.....	3
2.1 Potential Glare Sources.....	3
2.2 Potential Receptors.....	4
2.2.1 Typical Rectangular Airport Traffic Pattern.....	4
2.2.2 Overhead Traffic Pattern.....	5
2.2.3 Traffic Patterns Analyzed.....	5
3 Cumulative Glare Analysis.....	7
3.1 Data Collection.....	7
3.2 Geometric Glare Modeling.....	7
3.2.1 Software Overview.....	7
3.2.2 Analysis Setup.....	8
3.2.3 Analysis Parameters.....	9
3.2.4 Analysis Techniques.....	12
3.2.5 Limitations of the Geometric Analysis.....	13
3.3 Glare Analysis Results.....	13
3.3.1 Per-Project Glare Analysis Results.....	14
3.3.2 Per-Receptor Glare Analysis Results.....	15
3.3.3 Discussion of Results by Traffic Pattern.....	16
3.4 Multiple Sources of Glare.....	19
3.5 Conclusion.....	21
4 References.....	22
5 Document Preparers.....	24

TABLES

1 Projects Included in the Cumulative Analysis.....	3
2 Analyzed Traffic Patterns.....	5
3 Analysis Batches.....	8
4 Site Settings.....	9
5 Flight Path Receptor Analysis Names and Parameters.....	10

6 Per-Project Discrete Glare 14
 7 Per-Receptor Cumulative Glare Results 15

FIGURES

1 Analysis Study Area 26
 2 Comparison of Photovoltaic Tracking Systems 28
 3A Airport Receptor Locations – Runway 12 General Aviation Rectangular Traffic Pattern 30
 3B Airport Receptor Locations – Runway 30 General Aviation Rectangular Traffic Pattern 32
 3C Airport Receptor Locations – Runway 14 General Aviation Rectangular Traffic Pattern 34
 3D Airport Receptor Locations – Runway 32 General Aviation Rectangular Traffic Pattern 36
 3E Airport Receptor Locations – Runway 14 C-17/KC-135 Rectangular Traffic Pattern 38
 3F Airport Receptor Locations – Runway 32 C-17/KC-135 Rectangular Traffic Pattern 40
 3G Airport Receptor Locations – Runway 14 Overhead Traffic Pattern 42
 3H Airport Receptor Locations – Runway 32 Overhead Traffic Pattern 44
 4A Cumulative Glare Analysis Results – Runway 12 General Aviation Rectangular Traffic Pattern 46
 4B Cumulative Glare Analysis Results – Runway 30 General Aviation Rectangular Traffic Pattern 48
 4C Cumulative Glare Analysis Results – Runway 14 General Aviation Rectangular Traffic Pattern 50
 4D Cumulative Glare Analysis Results – Runway 32 General Aviation Rectangular Traffic Pattern 52
 4E Cumulative Glare Analysis Results – Runway 14 C-17/KC-135 Rectangular Traffic Pattern 54
 4F Cumulative Glare Analysis Results – Runway 32 C-17/KC-135 Rectangular Traffic Pattern 56
 4G Cumulative Glare Analysis Results – Runway 14 Overhead Traffic Pattern 58
 4H Cumulative Glare Analysis Results – Runway 32 Overhead Traffic Pattern 60
 5 Simulated Example of Cumulative Glare 62

APPENDIX

A Detailed Modeling Results

Acronyms and Abbreviations

Acronym/Abbreviation	Definition
ATCT	air traffic control tower
ALUC	County of Riverside Airport Land Use Commission
AOI	area of influence
FAA	Federal Aviation Administration
GIS	geographic information system
I	Interstate
OCR	optical character recognition
PV	photovoltaic
ZAP ID	zoning application identification number

INTENTIONALLY LEFT BLANK

1 Introduction

1.1 Purpose and Scope

The purpose of this Cumulative Glare Analysis Report (report) is to assess the potential for concurrent glare impacts associated with the development of rooftop solar photovoltaic projects within the area of influence (AOI) of March Air Reserve Base (MARB) in Riverside County, California.

This report assesses the collective potential for 26 previously approved rooftop solar projects to cast glare on sensitive receptors associated with flight operations at MARB including two active runways and the single air traffic control tower (ATCT). All of the projects included in this analysis had previously performed and submitted glare studies in accordance with County of Riverside Airport Land Use Commission (ALUC) requirements for approval. This analysis does not attempt to assess or call into question the validity of those previous analyses, but instead quantify their combined potential to cause glare impacts using uniform modeling parameters and methodology. See Figure 1, Analysis Study Area, for the project locations within the AOI of MARB.

In addition, this report does not attempt to qualify whether glare produced by photovoltaic (PV) systems is or is not a hazard to operations at airports like MARB. Instead, the goal of this report is to quantify the cumulative glare produced by the 26 projects analyzed and provide insight into when and where a cumulative glare effect might be experienced by personnel at MARB and what that effect might look like. Glare reflected from PV systems can be received by various ground-based receptors such as motorists and the public; however, this report focuses specifically on the effects to flight operations at MARB and does not attempt to quantify cumulative impacts to other land uses.

All the projects included in this analysis fall within the AOI and are off federal/U.S. Air Force property. Nevertheless, the analysis was conducted per Federal Aviation Administration (FAA) recommended procedures described in the Technical Guidance for Evaluating Selected Solar Technologies on Airports (FAA 2018); the geometric glare modeling software used adheres to FAA policy regarding solar energy system projects on federally obligated airports (86 FR 25801–25803).

This report includes an introduction to PV technologies and their potential to result in glare. Chapter 2, Source and Receptor Overview, provides a description of the projects included in the analysis, as well as the potential receptors associated with MARB, and Chapter 3, Cumulative Glare Analysis, describes the methodology used to perform the glare analysis and provides a summary of the analysis results. Chapter 4, References Reviewed, provides a list of the references cited in this report, and Chapter 5, Document Preparers, provides a list of those involved in the preparation of this report. Lastly, the complete detailed glare results generated by the modeling software are provided in Appendix A, Detailed Modeling Results.

1.2 General Concepts of Solar Technologies and Glare

All projects analyzed in this report involve the installation of PV panels to convert the sun's light into electrical energy. To increase the efficiency of this conversion process, designers of solar systems strive to maximize the amount of solar energy that can be absorbed by solar cells. Increased efficiency has the added benefit of reducing the amount of light that could potentially reflect off the solar panels. Reflected light can cause glint (a quick

reflection) and glare (reflection that lasts for a longer duration), which can create hazards for air-traffic-control personnel, motorists, and other potential receptors. For the purpose of this report, any light reflected off the solar panels or any other reflective surface is referred to as “glare.” These reflected beams of light that make up the glare are generally shaped like 3D cones extending from the source of the glare into infinity. The size, shape, and direction of this cone are a function of the angle of the solar panels relative to the sun’s location, as well as the texture of the material making up the surface of the solar panels.

There are several key design considerations that can reduce glare from solar panels. One of the main factors of reflectance is the position of the PV modules relative to the sun. A panel that has been designed to absorb 90% of the sunlight that directly meets the face of the panels (perpendicular to the sun’s rays) may have that absorption significantly reduced if the panel is not directly facing the sun (ForgeSolar 2023). Because the sun tracks across the sky over the course of a day, fixed-mount stationary panels can only maximize their efficiency for a few minutes out of the day when the sunlight is directly perpendicular to the face of the panel. To maximize the amount of solar energy generated from the solar array, some PV systems employ tracking mechanisms that adjust the angle of the panels to track the sun’s trajectory as it crosses the sky. Figure 2, Comparison of Photovoltaic Tracking Systems, provides an illustrative example of a fixed-mount panel system, single-axis tracking system, and dual-axis tracking system and their relative potential to create glare.

In addition to panel orientation, the materials used in the panel construction play an important role in reducing glare and maximizing efficiency. For example, different glass textures can be used to absorb light beams into the solar array, and anti-reflective coatings can be added to the glass to further reduce reflectivity at high-incidence angles (the angle at which the light hits the solar array)(Yellowhair 2015).

All the projects analyzed in this report utilized a fixed-mount system, as illustrated by the leftmost system in Figure 2. Generally, the panels are tilted to the south to reduce the angle of incidence of the incoming sunlight but remain in a fixed position relative to the earth’s surface. Because of this fixed alignment, the potential for these systems to generate glare will increase as the angle of incidence with the sun’s rays increases, resulting in a greater chance of glare in the mornings and evenings when the sun is closer to the horizon.

The surface texture of the panels and the presence/absence of antireflective coatings vary on a per-project basis. See Appendix A for information regarding the per-project material parameters used in the analysis.

Glare can result in visual hazards and temporary loss of vision (also known as flash blindness). The hazard level of glare depends on the ocular impact to the observer. Generally, an ocular impact is calculated as a function of the size of the glare spot and the intensity of the light. For the purpose of this report, an ocular impact is classified in one of three categories, as follows:

- **Green:** Low potential for the glare to cause an after-image
- **Yellow:** Potential to cause a temporary after-image
- **Red:** Potential to cause retinal burn and permanent eye damage

2 Source and Receptor Overview

2.1 Potential Glare Sources

A total of 26 previously approved rooftop solar PV projects were analyzed for this report, all of which are located within MARB's AOI. Distances from MARB to the projects vary significantly, with some projects located directly adjacent to the MARB property boundary while others are up to 3.5 miles away. A total of 17 of the projects are located within an unincorporated area of Riverside County to the west and southwest of MARB, with three of these projects also falling within the March Joint Powers Authority (JPA) Boundary. Four of the projects are located in the City of Perris to the south of MARB, and the remaining five projects are located within the City of Moreno Valley to the east and north of MARB.

The projects are identified in this report's text and figures using their county-assigned zoning application identification numbers (ZAP ID). The age of the permit applications for the 26 projects ranges from April 2016 at the earliest, to March 2023 at the most recent. Nearly all the PV arrays that were analyzed are mounted on or are planned to be mounted on large industrial warehouse buildings, in locations characterized by predominantly industrial land uses. See Table 1 for the ZAP ID, address, number of PV array groups, and approximate PV square footage for each project analyzed in this report. Each project analyzed is comprised of at least one PV array group, representing the outer boundary of the PV arrays, with some projects containing up to seven PV array groups. See Figure 1 for the location of each project, labeled by their ZAP ID number, as well as the MARB property boundary, JPA Boundary and AOI, with the surrounding cities of Riverside, Moreno Valley, Perris, Menifee, Canyon Lake, and Lake Elsinore.

Table 1. Projects Included in the Cumulative Analysis

ZAP ID	Address	No. of Panel Groups	Approximate Area of PV Modules (square feet)
1216	24300 Nandina Ave, Moreno Valley, CA	2	125,714 sq ft
1302	Southeast Corner of Placentia Ave and Harvill Ave, Perris, CA	1	93,009 sq ft
1314	22690, Cactus Ave, Moreno Valley, CA	7	38,762 sq ft
1371	Southwest Corner of Nandina Ave and Decker Rd, County of Riverside, CA	2	60,049 sq ft
1386	21362 Harvill, Perris, CA	1	200,218 sq ft
1388	24208 San Michele Rd, Moreno Valley, CA	2	559,071 sq ft
1391	Southeast Corner of Harley Know Blvd and Harvill Ave, Moreno Valley, CA	6	328,065 sq ft
1396	Northeast Corner of Placentia Ave and Patterson Ave, County of Riverside, CA	1	50,997 sq ft
1398	19972 Patterson Ave, Perris, CA	1	206,555 sq ft
1400	20463 Sharon Ann Ln, Perris, CA	1	38,063 sq ft
1404	4200 Webster Ave, Perris, CA	1	161,403 sq ft
1411	21600 Cactus Ave, Riverside, CA	2	326,360 sq ft

Table 1. Projects Included in the Cumulative Analysis

ZAP ID	Address	No. of Panel Groups	Approximate Area of PV Modules (square feet)
1421	Northwest Corner of Cajalco Rd and Harvill Ave, Perris, CA	1	209,299 sq ft
1425	21500 Harvill Ave, Perris, CA	1	226,105 sq ft
1458	14114 Business Center Dr, Moreno Valley, CA	1	19,200 sq ft
1462	14451 Commerce Center Dr, Moreno Valley, CA	1	15,405 sq ft
1488	Northeast Corner of Decker Rd and W Oleander Ave, County of Riverside, CA	1	311,653 sq ft
1493	19580 Seaton Ave, Perris, CA	1	325,200 sq ft
1509	15750 Meridian Pkwy, Riverside, CA	1	225,888 sq ft
1517	Northeast Corner of the Intersection of Harvill Ave, Cajalco Rd, Perris, CA	1	99,543 sq ft
1518	Southwest Corner of the Intersection of Harvill Ave and Water Street, Perris, CA	1	345,172 sq ft
1535	19115 Harvill Ave, County of Riverside, CA	1	25,327 sq ft
1541	South of Ramona Expressway, East of Nevada Road, Perris,, CA	1	621,695 sq ft
1558	14100 Meridian Pkwy, County of Riverside, CA	3	2,539 sq ft
1564	460 Harley Knox Blvd, Perris, CA	1	18,424 sq ft
1566	400 Harley Knox Blvd, Perris, CA	1	36,460 sq ft

The projects analyzed included other components that do not have potential for significant glare and therefore were not analyzed in this report. These components included but were limited to PV panel mounting brackets, electrical inverters, electrical conduits, alternating current disconnects, and PV production metering and control systems.

2.2 Potential Receptors

To ensure that land uses around the base are compatible with the base’s flight operations, MARB staff in conjunction with the ALUC have established a standard list of potential receptors to be analyzed for glare impact. These receptors include eight air traffic patterns associated with the two active runways on the base, and the single operating ATCT.

2.2.1 Typical Rectangular Airport Traffic Pattern

Traffic patterns are standardized flight paths around an airfield that help manage the flow of air traffic. They ensure that all pilots know what to expect in terms of other aircraft movements, making it easier to maintain safe distances and avoid collisions. A typical traffic pattern, known as a rectangular pattern, is made of five components: the upwind leg, the crosswind leg, the downwind leg, the base leg, and the final approach.

The first leg of a traffic pattern, the upwind leg, describes the aircraft’s movement immediately after takeoff, as the aircraft climbs straight along the extended centerline of the runway. Next, the during the crosswind leg, the aircraft

makes a 90-degree turn to the left or right, flying perpendicular to the runway. After another 90-degree turn, the aircraft will begin the downwind leg, flying parallel to the runway but in the opposite direction of landing or takeoff. At the base leg, the aircraft makes another 90-degree turn, this time flying perpendicular to the runway again, but aligned with the approach end of the pattern. When the pilot prepares for the final approach, they make one last 90-degree turn to align with the runway and follow a straight-in path to landing (FAA 2021).

2.2.2 Overhead Traffic Pattern

More commonly used in military aviation, overhead traffic patterns are designed to allow for faster aircraft to re-enter the pattern and land in a more expedient manner. This pattern is often used by faster aircraft to integrate into the airfield traffic pattern, it eliminates the crosswind and base legs of a rectangular pattern, leaving only three legs: the initial, the downwind, and the final.

On initial approach to an overhead pattern, the aircraft approaches the airfield at a higher altitude than the standard rectangular traffic pattern (500 feet higher in the case of MARB), usually aligned with the runway’s extended centerline. As the aircraft reaches a point above the runway’s threshold, it makes a quick 180-degree turn to the left or right (depending on the direction of traffic flow) and begins the downwind leg, traveling in the opposite direction of a landing. Instead of a separate base leg, the aircraft then makes a single continuous descending turn from the downwind leg to align with the runway and begins the final approach.

2.2.3 Traffic Patterns Analyzed

The traffic patterns included in the cumulative analysis describe the expected aircraft flight paths for general aviation and military grade aircraft. Each traffic pattern is made up of up to five 3D line segments, one segment for each leg of the traffic pattern. These 3D line segments are described by their starting and ending latitude, longitude, and elevation and were used to simulate the path along which an aircraft would typically be piloted while maneuvering an air traffic pattern. A total of 36 line segments were analyzed for this report. See Table 2 for their descriptions and line segment counts, as well as Figures 3A through 3H, Airport Receptor Locations, for maps of their locations.

Table 2. Analyzed Traffic Patterns

Pattern Description	Number of Line Segments Analyzed	See Figure
Runway 12 General Aviation Rectangular Traffic Pattern	5	3A
Runway 30 General Aviation Rectangular Traffic Pattern	5	3B
Runway 14 General Aviation Rectangular Traffic Pattern	5	3C
Runway 32 General Aviation Rectangular Traffic Pattern	5	3D
Runway 14 C-17/KC-135 Rectangular Traffic Pattern	5	3E
Runway 32 C-17/KC-135 Rectangular Traffic Pattern	5	3F
Runway 14 Overhead Traffic Pattern	3	3G
Runway 32 Overhead Traffic Pattern	3	3H

INTENTIONALLY LEFT BLANK

3 Cumulative Glare Analysis

In evaluating the potential cumulative glare effects on daily flight operations at MARB, Dudek staff applied a systematic multistep methodology. The process began with collecting data on the locations and specifics of the 26 PV array projects being analyzed and the locations of the potential receptors (i.e. flight paths and ATCT). This was followed by the implementation of an industry standard 3D geometric modeling tool to pinpoint and assess the glare potential at each project site. Finally, the output data from the modeling were processed, analyzed, and interpreted for this report.

3.1 Data Collection

At the outset of the cumulative analysis, ALUC staff provided Dudek with the glare analysis reports that had been submitted to the County of Riverside as part of the standard permitting process and a text file containing the precise coordinates of the flight path and ATCT receptors. The reports were provided to Dudek as PDFs. These 26 glare analysis reports, one for each project being analyzed, utilized the same geometric modeling software as was used in this cumulative analysis, making the transfer of parameters a relatively straightforward process.

The modeling parameters in the provided PDF reports describe the geometry of each PV array group (in latitude, longitude, and elevation coordinates), as well as the implementation details of each modeled array, such as PV module tilt, orientation, and material. With the help of optical character recognition (OCR) features available in Adobe Acrobat, Dudek staff was able to transfer the parameter data from the PDF documents into a Microsoft Excel spreadsheet.

The resulting spreadsheet contained hundreds of rows describing the precise location, size, and shape of the PV arrays, along with the other implementation parameters needed to perform the cumulative analysis. Dudek staff developed a Python programming script to convert the Excel spreadsheet into a file format that could be directly read by the glare modeling software. To further assist in the quality control checks on data entry, another Python script was developed to convert the PV array data into a 3D geographic information system (GIS) layer that could be overlaid on aerial imagery for visual confirmation. Because the data entry task utilized automated technologies, the number of errors detected in the data made up a very small percentage of the total and were mostly due to issues with the OCR process.

Another Python script was used to convert the air base flight path and ATCT receptors to a format that could be directly entered into the glare modeling software, as well as a GIS layer for mapping and quality control. Because these data originated in an easily processable digital format, the conversion process was entirely free of data entry errors.

3.2 Geometric Glare Modeling

3.2.1 Software Overview

For this analysis, Dudek staff used the industry standard GlareGauge by ForgeSolar, a 3D geometric glare analysis software tool used to disclose potential glare impacts associated with the operation of PV arrays. This software is based on Sandia National Laboratories' Solar Glare Hazard Analysis Tool, an FAA approved tool for modeling glare

on or near airports. With the Solar Glare Hazard Analysis Tool, standardized safety metrics define the anticipated glare intensity that would cause unwanted visual impacts to ATCTs and airplane pilots.

Glare intensity is described by the potential for after-image in the vision of the observer. Low potential for after-image is referred to as “green” glare, and potential for after-image is referred to as “yellow” glare. “Red” glare is representative of glare conditions with potential for permanent eye damage and is not typically possible for PV glare because PV arrays do not concentrate or focus reflected sunlight.

By inputting the solar panel locations and characteristics, as well as the locations and elevations of the receptors, the software can simulate the sun’s progression across the sky over the course of a year and model the potential glare caused by the proposed solar arrays. If glare is detected, the software can quantify the level of ocular impact hazard (green or yellow) and pinpoint the exact time of year the glare would occur. This analysis is automatically performed for every minute of the calendar year for each PV array and for each potential receptor defined in the model. See Section 3.2.5, Limitations of the Geometric Analysis, for more information about the known limitations in the modeling.

3.2.2 Analysis Setup

The glare analysis software has several constraints that had to be addressed before running the analysis. The software permits a maximum of 20 PV array groups per run of the analysis. Furthermore, these PV array groups must be geographically proximate, with all arrays situated within a 3-mile radius of each other. For the assessment of flight path receptors, the software has limits of a maximum of 20 distinct flight paths per run. Because the cumulative analysis covers 26 projects comprising 43 individual panel groups spread across an area of more than 9 miles and would need to be analyzed against 36 distinct flight paths, Dudek staff opted to break the analysis into six batches as described in Table 3. These six batches ensured that every PV array group was modeled against every airport receptor exactly once. The batch names correspond to the raw modeling outputs that can be found in Appendix A, which also provides details on the modeling parameters used for each modeled PV array group.

Table 3. Analysis Batches

Batch Name	ZAP IDs Included in Batch	Receptors Included in Batch
Northern Projects, Runway 12/30 with ATCT	1314, 1411, 1458, 1462, 1509, 1558	Flight Paths Associated with Runway 12/30 and the ATCT
Northern Projects, Runway 14/32	1314, 1411, 1458, 1462, 1509, 1558	Flight Paths Associated with Runway 14/32
Central Projects, Runway 12/30 with ATCT	1216, 1371, 1388, 1391, 1404, 1488, 1564, 1566	Flight Paths Associated with Runway 12/30 and the ATCT
Central Projects, Runway 14/32	1216, 1371, 1388, 1391, 1404, 1488, 1564, 1566	Flight Paths Associated with Runway 14/32
Southern Projects, Runway 12/30 with ATCT	1302, 1386, 1396, 1398, 1400, 1421, 1425, 1493, 1517, 1518, 1535, 1541	Flight Paths Associated with Runway 12/30 and the ATCT
Southern Projects, Runway 14/32	1302, 1386, 1396, 1398, 1400, 1421, 1425, 1493, 1517, 1518, 1535, 1541	Flight Paths Associated with Runway 14/32

3.2.3 Analysis Parameters

All six analysis batches utilized the same “Site Settings,” which GlareGauge uses to define the environmental parameters used in the analysis. The parameters used in this analysis are the default parameters recommended by ForgeSolar and required by regulatory authorities for analyzing hazards to airport receptors for projects on airport property. See Table 4 for the precise environmental parameters used, as well as a description of each parameter.

Table 4. Site Settings

Setting Name	Description	Value
Time Interval	The time step, or sampling interval, for the annual glare hazard analysis.	1 minute
Minimum Sun Altitude	Lower bound denoting the minimum altitude at which the sun is visible (year-round).	0 degrees
Peak DNI	The maximum direct normal irradiance (DNI) at the given location at solar noon. DNI is the amount of solar radiation received on a surface facing the sun during a 60-minute period. On a clear sunny day at solar noon, a typical peak DNI is approx. 1,000 watts per square meter (W/m ²).	1,000 W/m ²
DNI Varies?	If set to true, the peak DNI will be scaled at each time step according to the changing position of the sun and reduced DNI in the mornings and evenings.	TRUE
Sun angle (mrad)	The average subtended angle of the sun as viewed from earth is approx. 9.3 mrad or 0.5°.	9.3 mrad
Use enhanced subtended source angle calculation?	If set to true, the analysis will utilize improved computation of subtended source angle.	TRUE
Ocular Transmission Coefficient	Coefficient accounting for radiation that is absorbed in the eye before reaching the retina. A value of 0.5 is typical.	0.5
Pupil Diameter	Defines the diameter of the pupil of the observer receiving predicted glare. The size impacts the amount of light entering the eye and reaching the retina. A typical value for daylight adjusted eyes is 2 mm.	2 mm
Eye Focal Length	Distance between the nodal point (where rays intersect in the eye) and the retina. This value is used to determine the projected image size on the retina for a given subtended angle of the glare source. A typical eye focal length is 17 mm.	17 mm

The PV array group parameters used in this cumulative analysis, including PV array geometry and implementation details, were transferred from the original glare analysis reports provided by the ALUC and were only checked for consistency with those reports. Assessing the correctness or validity of those parameters was not within the scope of this analysis, and therefore not confirmed by Dudek staff before running the cumulative analysis. See Appendix A for the analysis parameters used for each PV array group.

Because the GlareGauge modeling software was intended specifically to address the FAA’s concerns regarding flights approaching airports, the software only includes functionality intended to model 2-mile direct flight approach paths to runway thresholds. These approach paths are the only supported way to model flight paths while retaining the ability to restrict the maximum downward and azimuthal (left-to-right) viewing angle of the pilot. Without these settings, modeled air traffic could potentially receive glare from sources that they couldn’t realistically see, such as PV arrays directly below or behind the airplane.

Since the flight paths provided by the ALUC describe flight paths for the entire flight pattern and not only the approach paths, Dudek staff chose to generate model configuration files that altered the 2-mile approach path receptor types from their intended use by manually setting their start and end coordinates to match those provided by the ALUC. Dudek staff confirmed that this methodology was valid by comparing the results of an analysis using modified 2-mile approach path receptors, with the results of an analysis that used standard route receptor lines. The results that utilized the standard route receptor lines without downward and azimuthal view restrictions yielded glare totals that were slightly greater than the results that did utilize view restrictions, as was expected.

The default maximum azimuthal view parameter for flight paths is set to 50 degrees, meaning that the pilot can receive glare from sources 50 degrees to the left or right of the center. This default is based on FAA research that determined that the impact of glare appearing beyond 50 degrees is mitigated because it is outside the peripheral view of a pilot focused on a runway directly in their line of travel (straight ahead) (ForgeSolar 2023). In this cumulative analysis, some of the flight path receptors are not approach paths, meaning the pilot’s attention would not necessarily be focused straight ahead, but could potentially be focused on air traffic or runway thresholds as much as 90 degrees to the left or right of center. For this reason, Dudek staff conservatively set the maximum azimuthal view of the pilot to 90 degrees for the crosswind, downwind, and base flight paths and retained the 50-degree setting for only those paths on direct approach to or take-off from a runway. Table 5 describes the parameters used for each of the 36 flight paths, as well as the short names that were used in the analysis software. A shortened name for each flight path receptor was needed due to software limitations; these are only used to reference the flight paths in the detailed modeling results found in Appendix A.

Table 5. Flight Path Receptor Analysis Names and Parameters

Flight Pattern Leg	Pilot Vertical View	Pilot Azimuthal View	Analysis Short Name
Runway 12 General Aviation Rectangular Traffic Pattern			
Upwind	30	50	FP11
Crosswind	30	90	FP08
Downwind	30	90	FP09
Base	30	90	FP07
Final	30	50	FP10
Runway 30 General Aviation Rectangular Traffic Pattern			
Upwind	30	50	FP16
Crosswind	30	90	FP13
Downwind	30	90	FP14
Base	30	90	FP12
Final	30	50	FP15

Table 5. Flight Path Receptor Analysis Names and Parameters

Flight Pattern Leg	Pilot Vertical View	Pilot Azimuthal View	Analysis Short Name
Runway 14 General Aviation Rectangular Traffic Pattern			
Upwind	30	50	FP31
Crosswind	30	90	FP28
Downwind	30	90	FP29
Base	30	90	FP27
Final	30	50	FP30
Runway 32 General Aviation Rectangular Traffic Pattern			
Upwind	30	50	FP36
Crosswind	30	90	FP33
Downwind	30	90	FP34
Base	30	90	FP32
Final	30	50	FP35
Runway 14 C-17/KC-135 Rectangular Traffic Pattern			
Upwind	30	50	FP21
Crosswind	30	90	FP18
Downwind	30	90	FP19
Base	30	90	FP17
Final	30	50	FP20
Runway 32 C-17/KC-135 Rectangular Traffic Pattern			
Upwind	30	50	FP26
Crosswind	30	90	FP23
Downwind	30	90	FP24
Base	30	90	FP22
Final	30	50	FP25
Runway 14 Overhead Traffic Pattern			
Initial	30	90	FP03
Downwind	30	90	FP01
Final	30	50	FP02
Runway 32 Overhead Traffic Pattern			
Initial	30	90	FP06
Downwind	30	90	FP04
Final	30	50	FP05

The single ATCT operating at MARB was included in this cumulative analysis as a point observer. The location and height of the ATCT cab was provided by the ALUC in latitude/longitude coordinates and in feet above ground level. Ground level elevation was obtained from the U.S. Geological Survey and was determined to be 1,510 feet above mean sea level. Modeled point receptors such as ATCTs can receive glare from any direction or distance.

3.2.4 Analysis Techniques

The GlareGauge modeling software outputs the results of the geometric analysis as one Excel workbook per PV array group, with each workbook containing a spreadsheet for each receptor impacted by that panel array group. Because there are 37 receptors (including the ATCT) and 43 individual panel groups included in this analysis, there could have been up to 1,591 spreadsheets output by the analysis software for this analysis. Since not all panel array groups were predicted to affect all receptors, only approximately 250 spreadsheets resulted from the glare analysis.

The spreadsheets output by GlareGauge include one row for every minute that glare was predicted to be generated by a panel array group towards a receptor. In addition, the spreadsheets contain columns that describe various information about that minute of glare, including the exact time the glare occurred (formatted as a date/time field); the estimated ocular hazard of the glare, either “1” for green or “2” for yellow; and other fields that were used to calculate the ocular hazard, such as the direct normal irradiance, retinal irradiance, and subtended glare angle. For this analysis the only information Dudek staff needed was the time glare occurred and the level of predicted glare hazard.

In order to examine the cumulative effects of all of the projects’ glare towards every receptor at MARB, Dudek staff had to combine the approximately 250 spreadsheets into one database table that could then be further analyzed as a whole. To accomplish this, Dudek staff created a Python script that combined all of the spreadsheets into one database table containing nearly 1.2 million rows of data.

As mentioned previously, some projects are comprised of up to seven panel groups. The number of panel groups associated with each project has little relationship to the size of the project and has more to do with the shape or layout of the proposed solar array, making the number of panel groups an arbitrary number to this analysis. Because the GlareGauge software counts each minute of glare per panel group, it is entirely possible for some projects to cast multiple minutes of glare (one for each panel group in the project) towards a receptor within 1 minute of elapsed time. This would essentially overestimate the number of minutes a pilot receives glare from a project, and potentially result in more glare minutes than there are daylight minutes in a year. To remedy this, Dudek staff eliminated any duplicate minutes of glare from a project towards a given receptor, resulting in a maximum of 1 minute of “discrete” glare between a project/receptor combination for any given minute of the year.

Conversely, to gauge the cumulative effect of the 26 projects on receptors at MARB, Dudek staff needed to quantify how many projects might cast glare towards the same receptor during the same minute of the year. This number is referred to in this report as the “source count,” or the count of sources predicted to cast glare onto a receptor in any given minute of the year. With 26 projects in this analysis, this number could range from “0,” meaning no projects are casting glare to a particular receptor in that minute, to “26,” meaning all projects are casting glare to a given receptor within that minute. To generate this number, Dudek staff tallied the number of records in the database that shared the same minute in time, the same ocular hazard, and the same receptor name. This resulted in a new table with roughly 411,000 records, each record containing the date/time field, receptor name, ocular hazard, and source count.

With this information, Dudek staff utilized Excel to generate charts depicting the average hours per day of glare that a given receptor might receive during a given month of the year. The bars of the charts were colorized to depict what time of day the glare was predicted to be received, either in the morning (sunrise to 9:59 a.m.), midday (10:00 a.m. to 1:59 p.m.), or evening (2:00 p.m. to sunset). All times are based on Pacific Standard Time or Coordinated Universal Time (UTC) 8. In addition to charts, Dudek staff created maps depicting each flight pattern analyzed and which projects were predicted to contribute the most glare to that flight pattern.

3.2.5 Limitations of the Geometric Analysis

The following are known limitations in the glare analysis software:

- The GlareGauge software was developed to support the FAA's recommended procedures described in the Technical Guidance for Evaluating Selected Solar Technologies on Airports and was not intended to gauge the potential cumulative effects of multiple off-airport solar projects on airport operations. Additional analysis might be necessary to better determine safe or acceptable thresholds for cumulative glare.
- The geometric modeling algorithm uses bounding polygons to represent PV array groups and therefore does not rigorously represent the detailed geometry of a PV array. Detailed features such as gaps between modules, variable height of the PV arrays within the bounding polygons, and support structures are not represented in the model and therefore could vary from real-life conditions.
- The geometric modeling algorithm does not account for intervening terrain, structures, or vegetation between the PV arrays and the receptors. This could result in more minutes of glare being predicted towards a receptor than is realistic.
- The geometric modeling software does not report length of the flight path that is affected by glare produced by a given PV array within a given minute, only whether a flight path is affected or not.

3.3 Glare Analysis Results

This cumulative glare analysis was conducted in compliance with the FAA's recommended procedures described in the Technical Guidance for Evaluating Selected Solar Technologies on Airports (FAA 2018), and the geometric glare modeling software used adheres to FAA policy regarding solar energy system projects on federally obligated airports (86 FR 25801–25803). This policy does not apply to the projects being analyzed in this report but was included in this reporting to describe the standard methodologies used to assess solar glare near operating airports. Specifically, the glare analysis and software quantify the level of ocular impact hazard (reported as green or yellow glare) and pinpoint the time of year the glare is likely to occur.

This report does not attempt to qualify whether glare produced by PV systems is or is not a hazard to operations at airports like MARB. Instead, the goal of this analysis is to quantify the cumulative glare produced by the 26 projects analyzed and provide insight into when and where a cumulative glare affect might be experienced by personnel at MARB and what that effect might look like.

The results of the glare analysis indicate that all 26 projects analyzed could result in green glare (low potential to cause an after image) towards some of the flight path receptors associated with daily operations at MARB. No yellow glare (potential to cause a temporary after image) was predicted towards any of the receptors at MARB and no glare of any level was predicted towards the single operating ATCT. This is consistent to the present Riverside County Airport Land Use Commission standards. These findings are generally in line with the previous analyses done for the projects. Any discrepancy between the previous analyses can likely be explained by changes in the Solar Glare Hazard Analysis Tool modeling algorithm since those results were initially published, as well as differences in the receptor parameters used for this report.

3.3.1 Per-Project Glare Analysis Results

Table 6 shows the total minutes of green glare predicted for each project. The “Discrete Green Glare” column describes how many minutes each project is predicted to cast green glare to any receptor at MARB. If the project is predicted to cast green glare on multiple receptors (flight paths) within the same minute, that minute is only accounted for once in this column. The “Average Concurrent Receptors” column describes how many receptors, on average, received glare from that project within the same minute. Numbers closer to 1 indicate that the project only cast glare towards one receptor at a time for most of the year. The “Maximum Concurrent Receptors” column describes the maximum number of receptors that received glare from that project during the same minute.

Table 6. Per-Project Discrete Glare

Project by ZAP ID	Discrete Green Glare (minutes per year)	Average Concurrent Receptors Affected	Maximum Concurrent Receptors Affected
1216	18,899	1.43	3
1302	38,652	1.20	2
1314	29,187	6.45	14
1371	33,024	2.16	6
1386	13,595	1.08	2
1388	14,771	2.43	6
1391	76,024	2.42	9
1396	33,216	1.17	2
1398	26,932	1.19	2
1400	31,712	1.17	2
1404	7,168	1.00	1
1411	35,263	1.17	3
1421	22,811	1.16	3
1425	11,855	1.06	2
1458	20,645	1.15	3
1462	32,353	1.04	2
1488	27,763	1.24	3
1493	29,320	1.17	2
1509	25,732	1.08	2
1517	19,545	1.21	3
1518	29,900	1.06	2
1535	29,851	1.30	3
1541	39,287	1.33	3
1558	15,630	3.43	6
1564	14,622	2.01	4
1566	11,127	2.02	5

3.3.2 Per-Receptor Glare Analysis Results

To assess the cumulative effects of the 26 PV projects on receptors at MARB, Dudek staff first had to quantify both the total minutes of glare received by each flight path, as well as the number of projects that contributed to that glare. As mentioned previously, all 26 projects are predicted to cast glare towards receptors at MARB, but not all receptors at MARB were equally affected by those projects. Per the results, out of the 36 flight path receptors analyzed, 28 were predicted to receive glare from any of the projects. Table 7 details which receptors received glare and the total minutes of discrete glare received. In addition to that total, an “Average Concurrent Source Count” describes, on average, how many projects are predicted to cast glare on that receptor at any given time during the year (excluding the times of year where no glare is predicted). Similarly, a maximum concurrent source count is included to illustrate which receptors are predicted to be affected by the most projects during a single moment in time that glare is predicted.

Table 7. Per-Receptor Cumulative Glare Results

Flight Pattern Leg	Discrete Green Glare (minutes per year)	Average Concurrent Source Count	Maximum Concurrent Source Count
Runway 14 Overhead Traffic Pattern			
Initial	37,284	1.37	3
Downwind	0	0.00	0
Final	14,405	1.07	2
Runway 32 Overhead Traffic Pattern			
Initial	62,043	3.06	10
Downwind	43,291	3.30	8
Final	18,433	1.46	3
Runway 12 General Aviation Rectangular Traffic Pattern			
Upwind	2,612	1.00	1
Crosswind	0	0.00	0
Downwind	15,586	1.44	3
Base	9,168	1.22	2
Final	0	0.00	0
Runway 30 General Aviation Rectangular Traffic Pattern			
Upwind	841	1.00	1
Crosswind	0	0.00	0
Downwind	0	0.00	0
Base	7,809	1.00	1
Final	2,784	1.00	1
Runway 14 C-17/KC-135 Rectangular Traffic Pattern			
Upwind	1,768	1.44	2
Crosswind	28,479	1.26	3
Downwind	5,090	1.00	1
Base	13,053	1.26	4
Final	11,350	1.13	2

Table 7. Per-Receptor Cumulative Glare Results

Flight Pattern Leg	Discrete Green Glare (minutes per year)	Average Concurrent Source Count	Maximum Concurrent Source Count
Runway 32 C-17/KC-135 Rectangular Traffic Pattern			
Upwind	7,534	1.00	2
Crosswind	0	0.00	0
Downwind	38,537	4.30	12
Base	4,711	1.00	1
Final	15,899	1.59	4
Runway 14 General Aviation Rectangular Traffic Pattern			
Upwind	4,044	1.44	2
Crosswind	3,937	1.00	1
Downwind	113	1.00	1
Base	8,277	1.00	1
Final	0	0.00	0
Runway 32 General Aviation Rectangular Traffic Pattern			
Upwind	0	0.00	0
Crosswind	2,523	1.00	1
Downwind	34,625	1.88	5
Base	82	1.00	1
Final	16,569	1.26	3

3.3.3 Discussion of Results by Traffic Pattern

Runway 12 General Aviation Rectangular Traffic Pattern

This traffic pattern is expected to receive a moderate amount of green glare, with a total of approximately 27,000 minutes per year. As shown in Figure 4A, Cumulative Glare Analysis Results – Runway 12 General Aviation Rectangular Traffic Pattern, the most affected legs are the base and downwind legs. Both of these legs of the pattern experience glare in the late afternoon hours of the spring and summer months, averaging between 1 and 2 hours per day.

This pattern does not experience a significant cumulative effect from the 26 projects analyzed, with only one or two of those projects contributing glare at any time.

Runway 30 General Aviation Rectangular Traffic Pattern

This traffic pattern received the least amount of green glare of all the traffic patterns analyzed, at approximately 11,500 minutes per year total. As shown on Figure 4B, Cumulative Glare Analysis Results – Runway 30 General Aviation Rectangular Traffic Pattern, most of the glare predicted to be received by this traffic pattern was on the base leg, which for most of the year receives less than 20 minutes of glare per day, exclusively in the daylight evening hours. The upwind and final legs of the pattern receive less than 30 minutes per day, restricted to the

evening hours of a select few months of the year. This pattern also experiences the least cumulative effect, receiving glare from only one project at a time.

Runway 14 General Aviation Rectangular Traffic Pattern

As shown in Figure 4C, Cumulative Glare Analysis Results - Runway 14 General Aviation Rectangular Traffic Pattern, this traffic pattern is expected to receive relatively little green glare, at nearly 16,300 minutes per year. Glare towards any leg of this traffic pattern is predicted to stay below 1 hour per day, on average. The base leg of this pattern is predicted to receive the most glare, at 8,277 minutes per year, occurring primarily in the morning hours of the summer and winter months.

The upwind and crosswind legs of this pattern are both predicted to receive roughly 4,000 minutes of green glare per year. They both receive glare in the late winter and early fall months, with the upwind leg receiving glare in the morning and the crosswind leg receiving glare in the evening.

The downwind leg only receives a handful of minutes of glare per day on average in June, and the final leg is predicted to receive no glare. The cumulative effect on this traffic pattern is relatively low, with most legs of the pattern receiving glare from only one project at a time, with the exception of the upwind leg, which receives glare from two projects at a time in February and October.

The reason for the relatively low glare prediction for this pattern is the short length of the legs of the pattern when compared to the military aircraft patterns, which tend to be longer, as well as the lower count of PV projects that intersect the lines of flight.

Runway 32 General Aviation Rectangular Traffic Pattern

As shown on Figure 4D, Cumulative Glare Analysis Results - Runway 32 General Aviation Rectangular Traffic Pattern, this traffic pattern is expected to receive approximately 53,800 minutes of green glare per year from the 26 projects analyzed. The majority of the glare is received by the downwind leg of this pattern, with between 1 and 2 hours of glare per day on average. All the glare towards this leg is received in the morning hours, and the average source count hovers around two for most of the year. Glare towards the downwind leg comes mainly from the projects directly in the flight line, west of MARB and west of Interstate (I) 215, with some additional glare being received from the projects east/southeast of MARB.

The final approach of this pattern also receives between 1 and 2 hours of green glare per day, on average, occurring in the evening hours from April through August. The source count for glare on this leg stays between 1 and 1.5 on average and is generated by projects to the west-southwest of MARB, the same projects that generate most of the glare for the downwind leg.

The crosswind leg also receives afternoon glare, ranging between 15 and 45 minutes of green glare per day on average, but only during the months of May, June, and July. The glare directed towards this leg is predicted to come from only one source, ZAP ID 1411.

The base leg receives just a few minutes of glare per day on average, and only during the months of December and January, while the upwind leg is predicted to receive no glare year-round.

Runway 14 C-17/KC-135 Rectangular Traffic Pattern

As shown of Figure 4E, Cumulative Glare Analysis Results - Runway 14 C-17/KC-135 Rectangular Traffic Pattern, this traffic pattern receives almost 60,000 minutes of green glare per year, with nearly half of that glare being received in the crosswind leg. This leg of the pattern experiences between 1 and 2 hours of glare per day, on average, primarily in the evening hours, with less glare being received in the winter months. This glare is caused by the high density of projects to the southwest of MARB, west of I-215. As aircraft following this leg of the traffic pattern are flying west, into the setting sun, the projects directly off the right side of the aircraft are predicted to reflect some of that light into the line of flight. At any given time, this glare is expected to come from between one and two sources on average, peaking at three sources at select times in June.

The upwind, downwind, base, and final legs of this traffic pattern receive between 0.5 and 1.5 hours of green glare per day, on average, with that glare occurring in the morning hours of the fall and winter months, with the exception of the downwind leg, which receives morning glare in during the summer months. The source count for these legs of the pattern typically stays in the low digits between one and two, occasionally receiving glare from up to four sources on the base leg of the pattern in February. Glare towards the base and final leg of this pattern is due to the projects directly north/northeast of MARB.

Runway 32 C-17/KC-135 Rectangular Traffic Pattern

This traffic pattern receives approximately 66,500 minutes of glare per year. As shown on Figure 4F, Cumulative Glare Analysis Results - Runway 32 C-17/KC-135 Rectangular Traffic Pattern, the downwind leg receives almost 60% of the total glare of this pattern, exclusively in the morning hours. Glare towards the downwind leg is predicted to occur for between 1 and 2.3 hours per morning, with the shortest durations occurring in the winter months and the longest durations in May through August. This leg experiences the largest cumulative effect of the analysis, receiving glare from between 3 and 5 projects at a time for most of the year, peaking at 12 projects in at very select times in the winter months. The high levels of glare towards this leg are due to its relatively long length and the fact that the direction of flight lines up with the area of highest density of projects in the area to the southwest of MARB, west of I-215.

The final leg of this pattern receives nearly 16,000 minutes of glare per year, averaging between 1 and 2 hours per day in the evenings of the spring and summer months. The analysis predicts that, as aircraft are approaching runway 32, they will receive glare from between one and two projects, on average, off the lefthand side of the aircraft in the same direction as the setting sun.

The upwind leg of this pattern is predicted to receive between 0.5 and 1.5 hours of glare per day, on average, in the evenings of the spring and summer months, while the base leg is predicted to receive less than 1 hour of glare per day in the midday hours of May, June, and July. Both of these legs are predicted to only receive glare from one source at a time. The crosswind leg of this pattern is not predicted to receive any green glare.

Runway 14 Overhead Traffic Pattern

Per the results of the cumulative analysis and as shown on Figure 4G, Cumulative Glare Analysis Results – Runway 14 Overhead Traffic Pattern, this traffic pattern is predicted to receive approximately 37,000 minutes of green glare on the initial leg of the pattern, no glare on the return downwind leg, and then an additional approximately 14,000

minutes per year on the final approach to runway 14. This glare is expected to occur mainly in the fall and winter months, throughout the day, though on the final approach, glare is expected to be limited to the morning hours.

The glare towards this pattern is usually generated by only one or two projects at a time and is predominantly due to the projects to the north and east of MARB.

Runway 32 Overhead Traffic Pattern

This traffic pattern is expected to receive the most minutes of green glare per year out of all the traffic patterns analyzed, with approximately 123,000 minutes of green glare received by receptors in this pattern per year. As shown on Figure 4H, Cumulative Glare Analysis Results – Runway 32 Overhead Traffic Pattern, as aircraft approach the overhead pattern from the south on the initial leg, they will receive between 2 and 3.5 hours per day of green glare, throughout the year. This glare will occur almost exclusively in the evening hours and can be attributed to the large number of projects to the south/southwest of MARB, west of I-215. When glare is received by this flight path, it will be originating from between three and four different projects at a time.

Conversely, on the return downwind leg of this flight path, glare will be received in the morning hours throughout the year, averaging between 1 and 2.5 hours per morning. The morning occurrence of glare on this leg of the flight pattern is due to all of the projects being on the east side of the flight path. The modeling predicts that, on average, between two and four projects could produce glare towards this flight path at a time.

The final approach to this traffic pattern could experience up to 2 hours of green glare per day in the summer evenings, but this approach will experience a lesser cumulative effect than the other legs of this pattern, with only one to two projects contributing glare at any given time. This is likely due to this leg of the pattern being positioned to the north of many of the projects.

3.4 Multiple Sources of Glare

While this report does not attempt to make a qualitative determination on the severity of impacts due to PV glare on flight path receptors at MARB, it does aim to present a comprehensive overview of what the glare from the 26 projects analyzed might look like to pilots navigating the various traffic patterns at MARB. The challenge of this task lies in addressing the multiple dimensions of glare effect, including intensity, spatial coordinates, elevational differences, and temporal factors. A pilot following a path of a particular leg of a flight pattern will be traveling through all these dimensions, experiencing varying degrees of the effects of glare during their navigational course. This section will attempt to illustrate what it might look like from a pilot's point of view as they travel in and out of a beam of light reflected from a solar array and how multiple sources of glare might also affect this traversal.

To assist in describing the potential effect of multiple sources of glare towards flight receptors at MARB, Dudek staff selected one example flight path that exhibited a range of cumulative glare effects. The downwind leg of the Runway 32 C-17/KC-135 rectangular traffic pattern was selected because of its relatively high duration of morning glare during the summer months, as well as the relatively high average source count predicted for that leg. It would typically take between 2 and 3 minutes for an aircraft to travel the length of this leg, so a representative 3-minute period of time was selected that would provide representative example of cumulative glare.

On the summer solstice (June 21, 2023), between 6:41 a.m. and 6:43 a.m., the downwind leg of the flight pattern receives glare from nine concurrent sources for all 3 minutes. As shown in Figure 5, Simulated Example of

Cumulative Glare, an aircraft starting at the beginning of the leg on June 21 at 6:41 a.m. (labeled as Viewpoint #1) and traveling along the downwind flight path is predicted to receive no glare for that first minute of travel. The simulated view of Viewpoint #1 shows no sources of glare within the pilot's frame of view. This is because, as the sun rises at an azimuth of approximately 76 degrees (east-northeast) at that time, the light rays bounce off the panels at an angle that does not intersect the northern half of that leg of the pattern. These reflected beams of light that make up the glare are shaped like 3D cones extending into infinity, with the point of the cone starting at the surface of the PV array. Wherever these cones intersect the flight path in 3D space, glare will occur.

As the plane continues to travel south for about 1.5 minutes, it will first enter the glare cone of ZAP ID 1216. From the perspective of the pilot, a bright light will slowly appear on the left side of the aircraft. Though the flight path is still receiving glare from nine sources during this minute, only one source is affecting the pilot at this precise location. As the plane approaches Viewpoint #2, a second bright light off the left-hand side of the cockpit will appear, this time from ZAP ID 1371. This is simulated in the middle image on Figure 5. Now two separate projects are creating glare cones that are intersecting Viewpoint #2. As the plane continues to travel south for another 30 seconds, those two sources of glare will slowly fade, starting with ZAP ID 1216 and then ZAP ID 1371.

As the plane continues south for another minute, it will enter and exit the glare cone created by ZAP ID 1535. Again, this will appear to the pilot as a reflected light source off the left-hand side of the aircraft, slowly appearing and then disappearing. As the plane reaches Viewpoint #3, it will first enter the glare cone of ZAP ID 1421, followed by ZAP ID 1493 a few seconds later. Because ZAP ID 1493 is closer and larger than any of the glare sources experienced along this leg so far, it is likely going to be the brightest source of glare from the pilot's perspective. This is illustrated in the simulated view shown on the bottom image on Figure 5.

As the aircraft passes Viewpoint #3, it will enter and exit the glare cone of ZAP ID 1398 and then enter the glare cones of ZAP IDs 1396, 1400, and 1302. At this point, while within these glare cones, the aircraft will begin its turn to the base leg of the flight pattern and slowly exit all of the glare cones shown on Figure 5.

It is important to note that ocular hazard from multiple distinct sources towards a flight path is not likely to be additive, meaning that multiple sources of concurrent glare in the green ocular hazard category will not likely add up to glare in the yellow ocular hazard category. This is due to the way the ocular hazard is calculated as a function of the retinal irradiance (the intensity of light hitting the retina) and the diameter of the glare spot on the retina. For a given glare intensity, a smaller glare spot will result in a smaller glare intensity (Ho 2011).

A pilot traveling a flight path might experience multiple points of glare on different areas of their retina at different times over the course of their travel, but those points of glare will likely not be seen as a single larger point of glare in their vision unless the PV arrays from the multiple projects occupy the same uninterrupted surface (rooftop) and are utilizing the same tilt and orientation. A larger, uninterrupted, set of PV arrays utilizing the same parameters will have more potential to increase the size of the glare spot, thus increasing the ocular hazard. For this reason, projects that propose to expand their footprint on a given rooftop should be required reanalyze the project as-a-whole for glare.

As illustrated in this section, the impact of glare on an aircraft has a temporal as well as spatial component to it. Glare received by a flight path receptor will only affect an aircraft as it travels through that cone of glare, and that duration of effect will be dictated by the speed of the aircraft and the size of the cone of glare. Multiple sources of glare towards a flight path will result in either staggered or overlapping cones of glare, which will appear to the pilot as separate sources of light that will fade in and fade out as the aircraft travels into and out of each cone of glare.

3.5 Conclusion

This report assesses the collective potential for 26 previously approved rooftop solar projects to cast glare on sensitive receptors associated with flight operations at MARB including two active runways and the single ATCT. It does not attempt to qualify whether glare produced by PV systems is or is not a hazard to operations at airports like MARB. Instead, the goal of this report is to quantify the cumulative glare produced by the 26 projects analyzed and provide insight into when and where a cumulative glare affect might be experienced by personnel at MARB and what that effect might look like.

The per-receptor cumulative glare results predict that none of the receptors analyzed will receive yellow glare (potential to cause after image), but they do indicate that every flight pattern will receive some amount of green glare. The ATCT was not predicted to receive glare at any intensity level. It has also been made evident that there is a wide range of total glare minutes predicted for the eight flight patterns analyzed, from approximately 11,000 minutes predicted for the Runway 30 General Aviation Rectangular traffic pattern, up to roughly 123,000 minutes of green glare for the Runway 32 Overhead traffic pattern.

As expected, the analysis shows that, as the number of projects increase within the AOI of MARB, the potential for intersections between glare cones and flight paths will increase. In addition, because the implementation details of each project differ from one another in panel location, elevation, tilt, orientation, and build material, their glare cones will more likely intersect flight paths at different times of day and year, essentially spreading out the potential effects. A single leg of a flight path might receive glare from over a dozen different sources over the course of the year, but the glare cones from those sources often do not intersect simultaneously with an aircraft traveling along that flight path.

The analysis confirms that the number of sources of glare adjacent to MARB does not influence the overall glare intensity; two separate sources of green glare do not add up to a yellow glare hazard. Instead, as the number of green glare sources increases, so too will opportunities for glare to intersect with a flight path or ATCT at MARB.

4 References

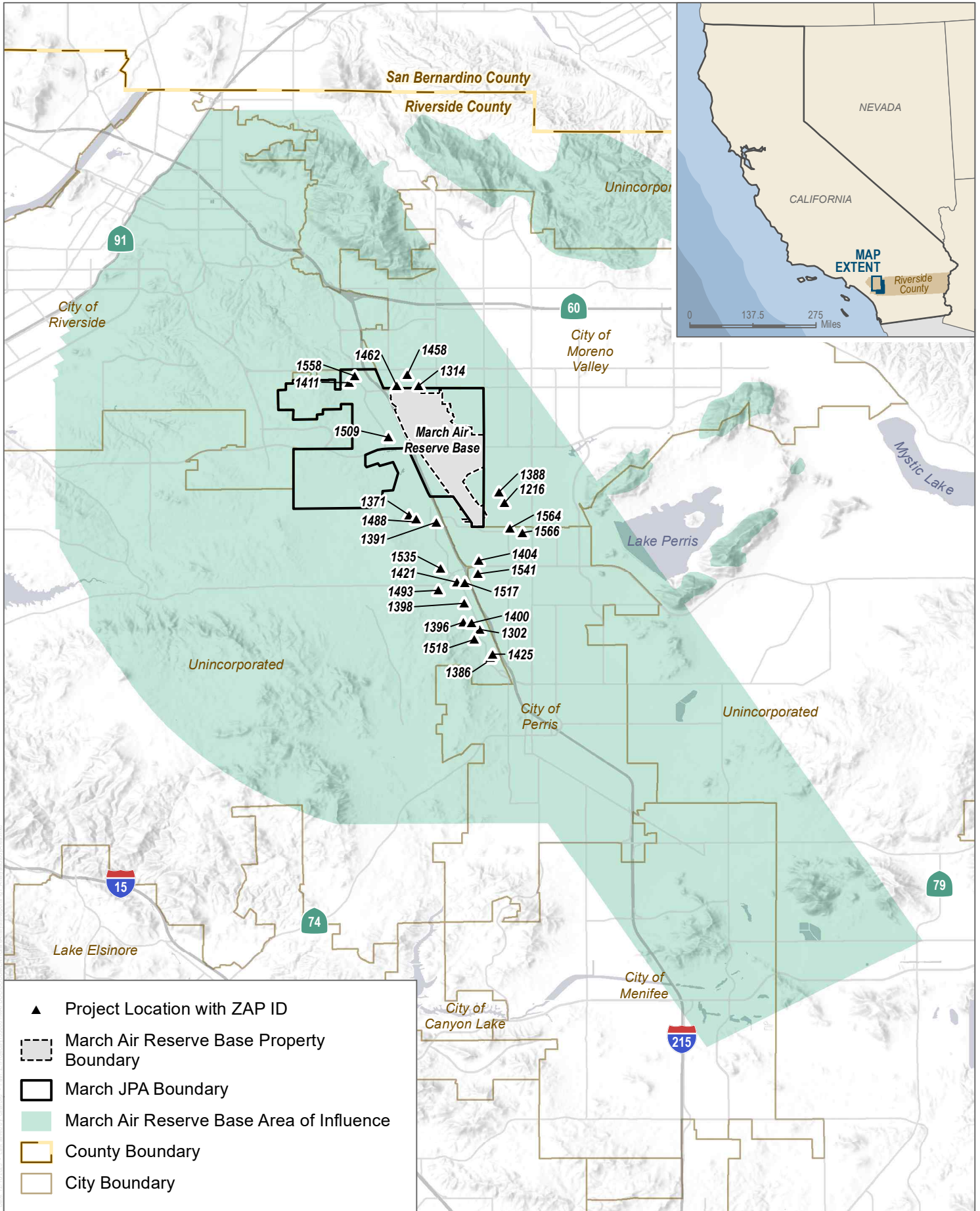
- FAA (Federal Aviation Administration). 2018. *Technical Guidance for Evaluating Selected Solar Technologies on Airports*. Version 1.1. Washington, DC: FAA, Office of Airports, Office of Airport Planning and Programming. April 2018.
- FAA (Federal Aviation Administration). 2021. *Airplane Flying Handbook*. Washington, DC: FAA, Flight Standards Service. 2021.
- ForgeSolar (ForgeSolar: PV Planning & Glare Analysis). 2023. "ForgeSolar Help." <https://www.forgesolar.com/help/>.
- Ho, C. K., Ghanbari, C. M., & Diver, R. B. (2011). Methodology to assess potential glint and glare hazards from concentrating solar power plants: Analytical models and experimental validation. *ASME Journal of Solar Energy Engineering*, 133.
- Yellowhair, J., & Ho, C. K. (2015). Assessment of photovoltaic surface texturing on transmittance effects and glint/glare impacts. In *ASME 2015 9th International Conference on Energy Sustainability collocated with the ASME 2015 Power Conference, the ASME 2015 13th International Conference on Fuel Cell Science, Engineering and Technology, and the ASME 2015 Nuclear Forum*. American Society of Mechanical Engineers.

INTENTIONALLY LEFT BLANK

5 Document Preparers

This report was prepared by Christopher Starbird.

INTENTIONALLY LEFT BLANK

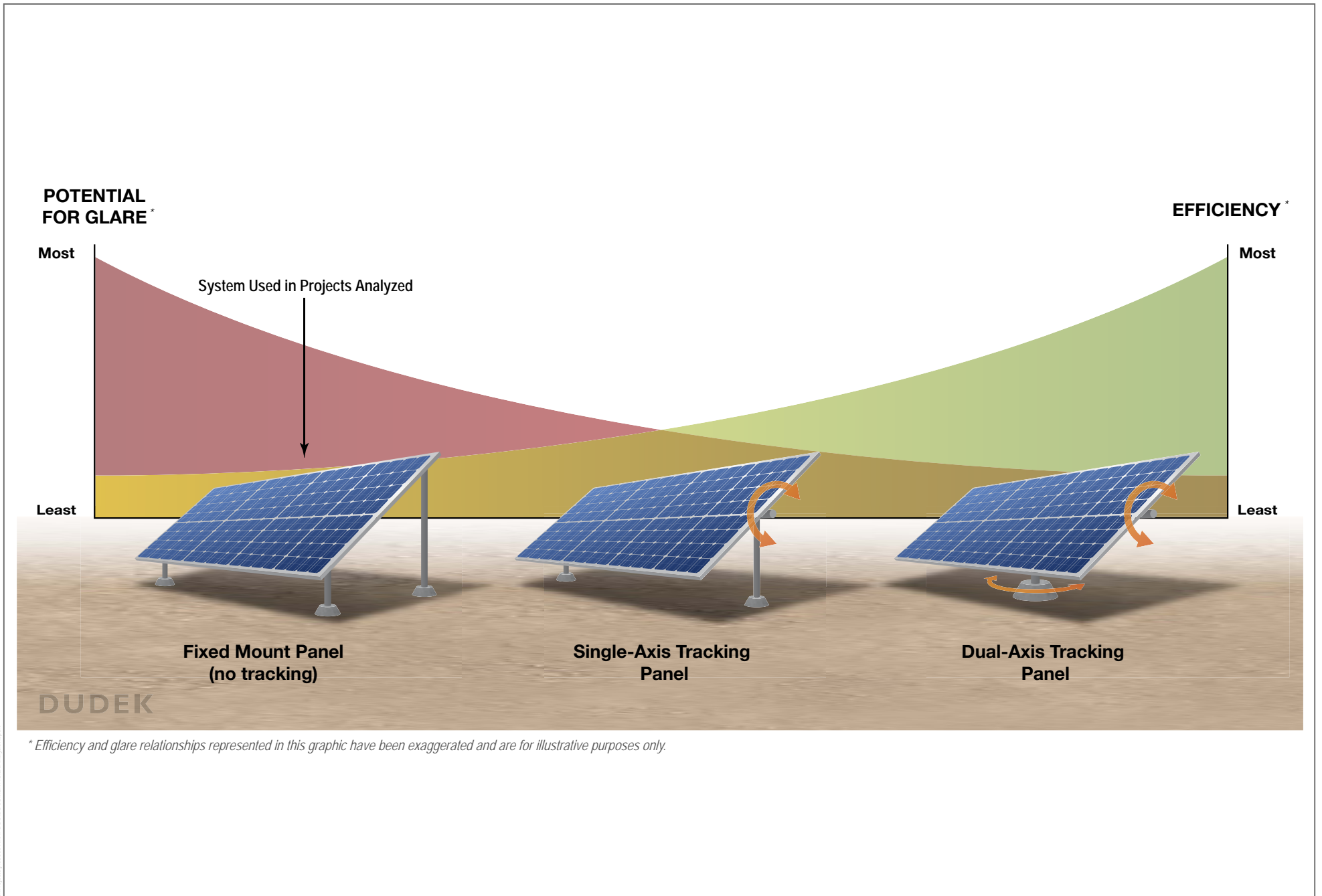


SOURCE: Esri and Digital Globe 2023

FIGURE 1

Analysis Study Area

INTENTIONALLY LEFT BLANK

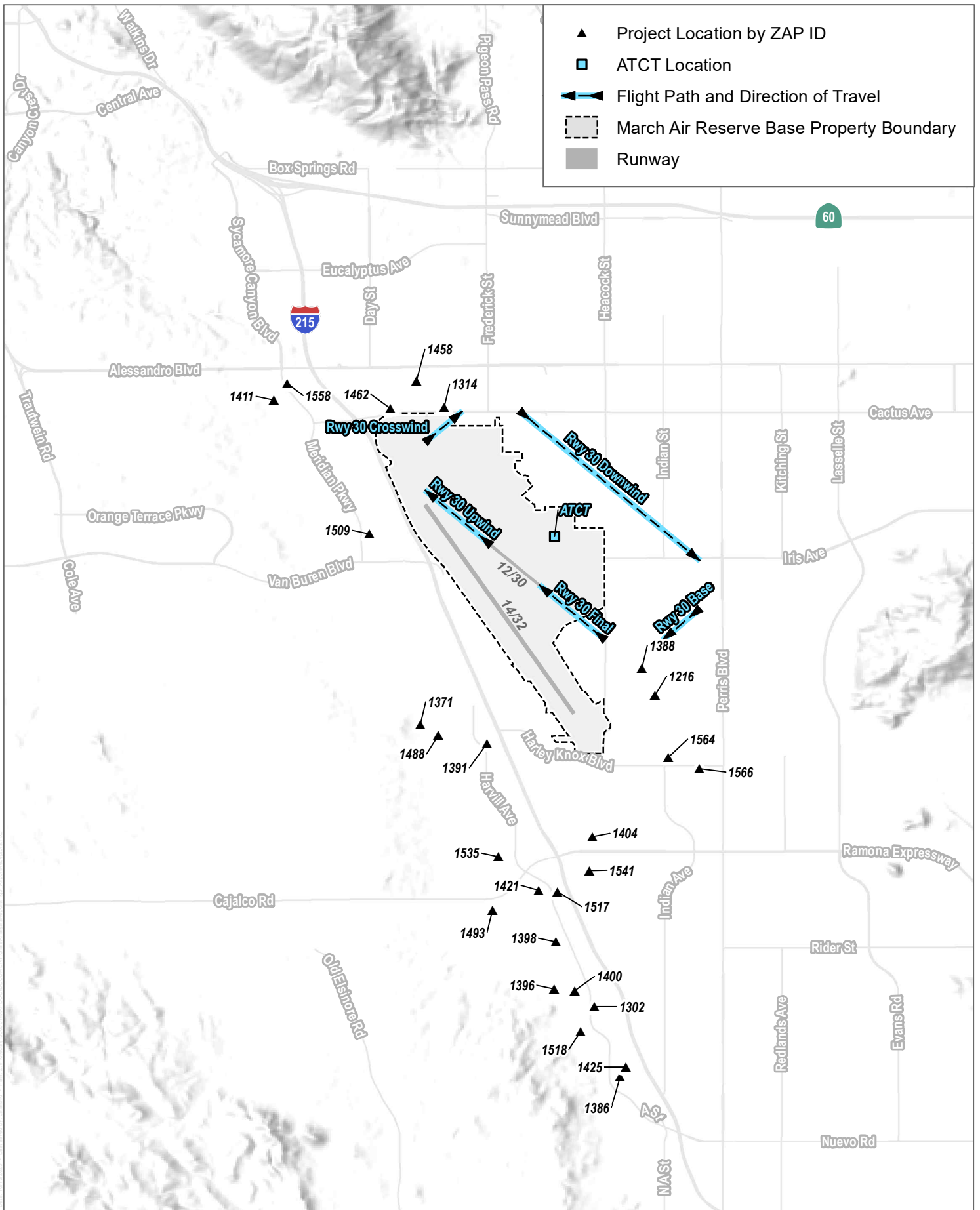


SOURCE: DUDEK 2023

FIGURE 2

INTENTIONALLY LEFT BLANK

INTENTIONALLY LEFT BLANK



SOURCE: Esri and Digital Globe 2023

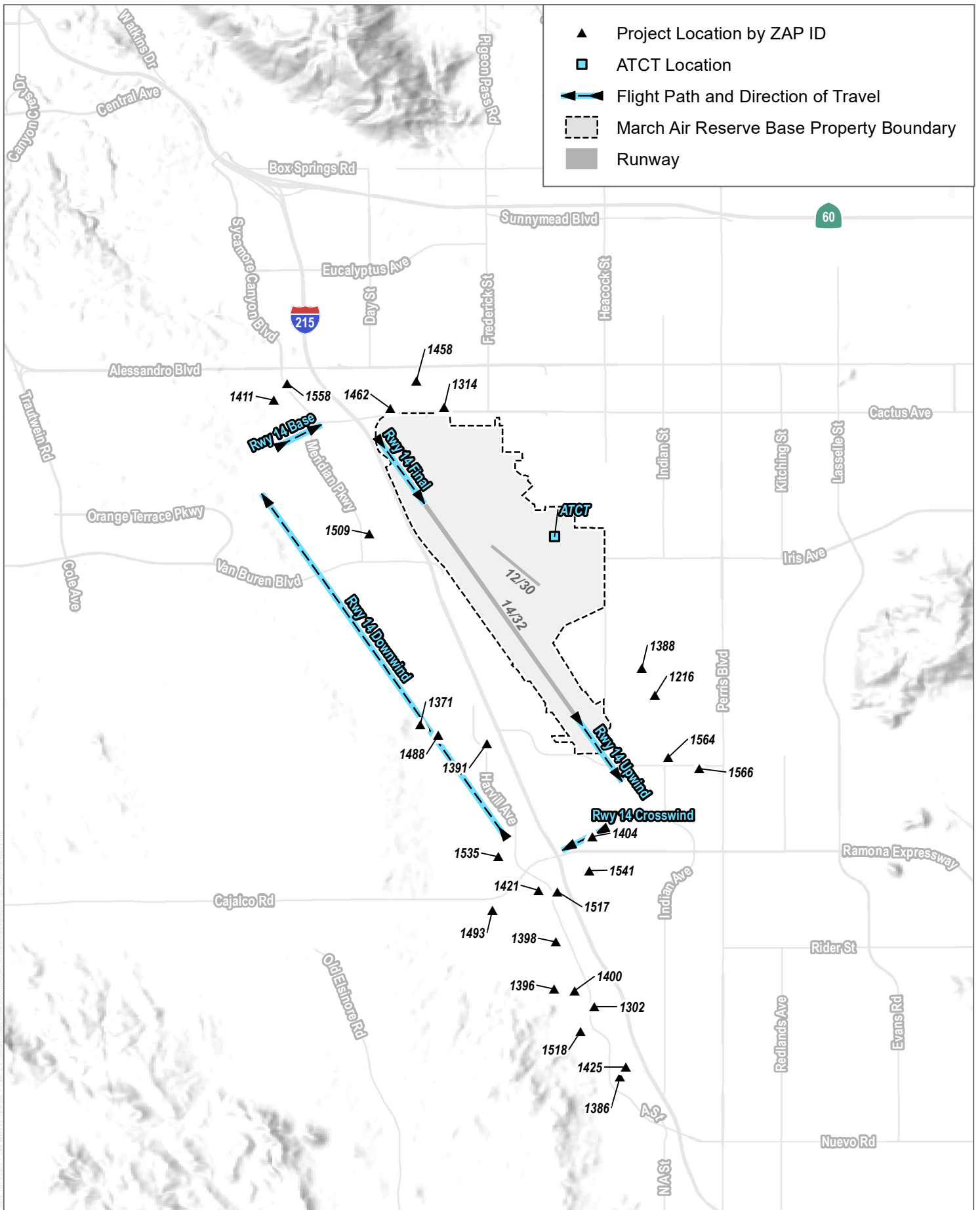
FIGURE 3B

Airport Receptor Locations - Rwy 30 GA Rectangular Traffic Pattern

March Air Reserve Base Compatible Use Study, Cumulative Glare Analysis



INTENTIONALLY LEFT BLANK



SOURCE: Esri and Digital Globe 2023

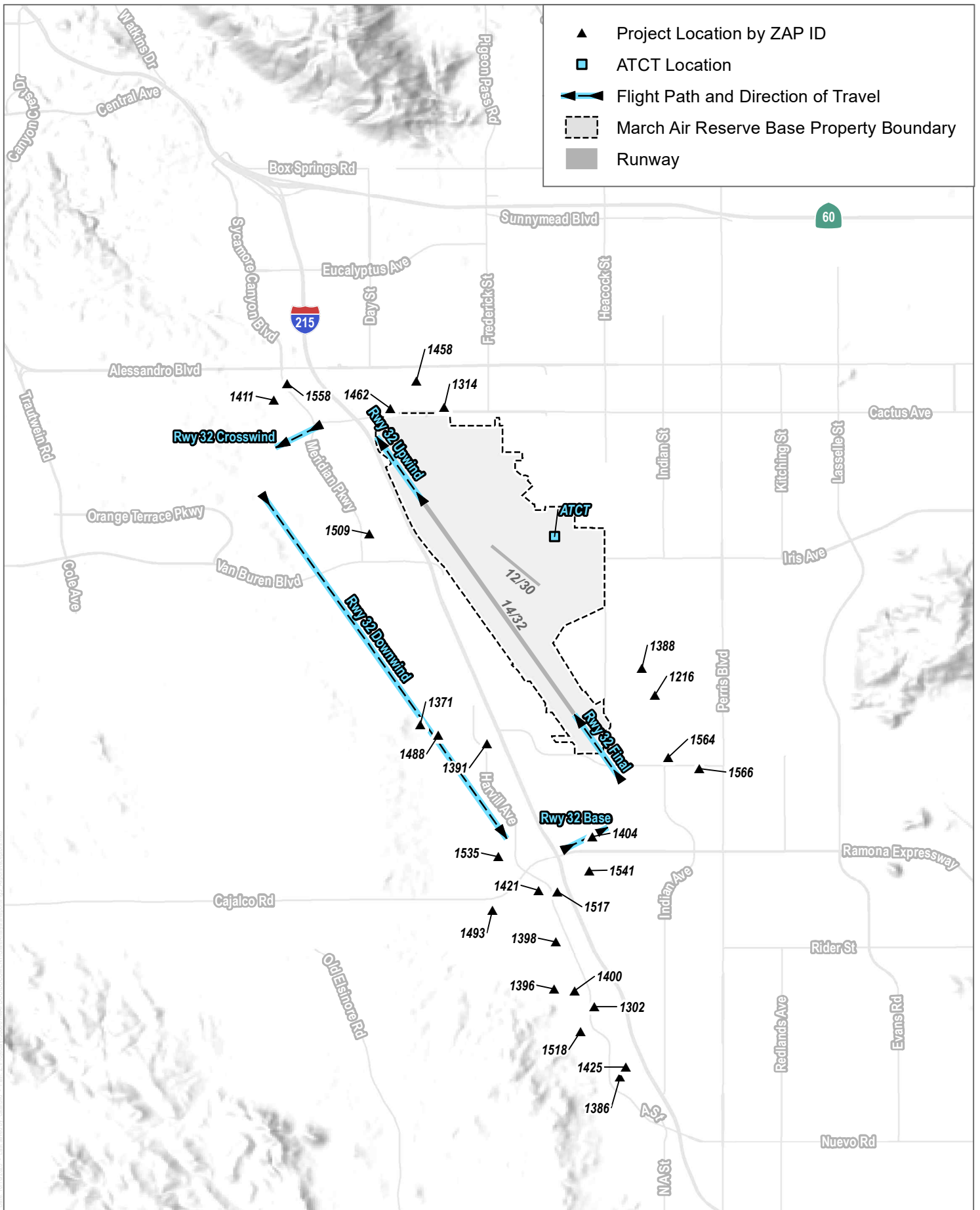
FIGURE 3C

Airport Receptor Locations - Rwy 14 GA Rectangular Traffic Pattern

March Air Reserve Base Compatible Use Study, Cumulative Glare Analysis



INTENTIONALLY LEFT BLANK



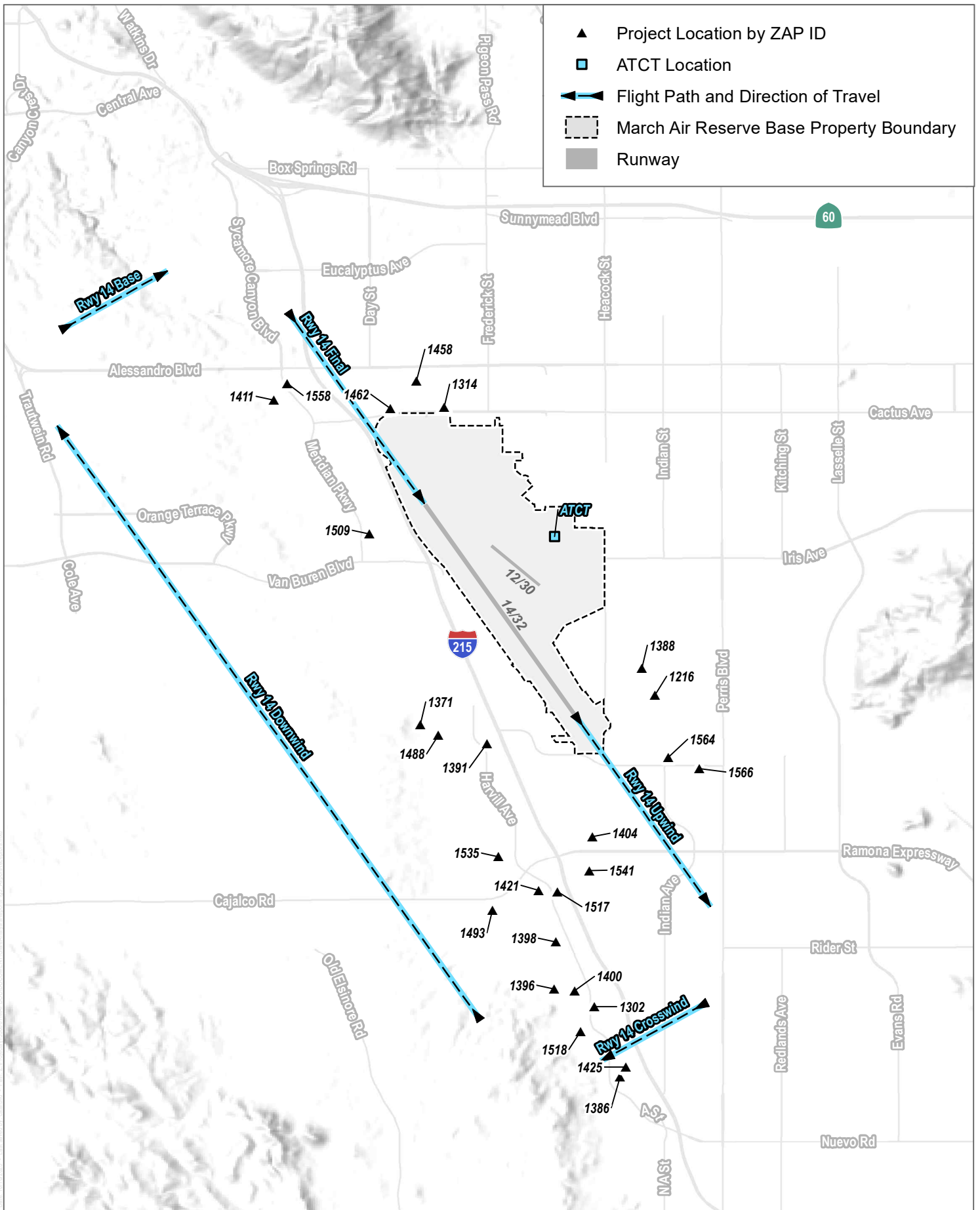
SOURCE: Esri and Digital Globe 2023

FIGURE 3D

Airport Receptor Locations - Rwy 32 GA Rectangular Traffic Pattern

March Air Reserve Base Compatible Use Study, Cumulative Glare Analysis

INTENTIONALLY LEFT BLANK



- ▲ Project Location by ZAP ID
- ATCT Location
- ↔ Flight Path and Direction of Travel
- March Air Reserve Base Property Boundary
- Runway

SOURCE: Esri and Digital Globe 2023

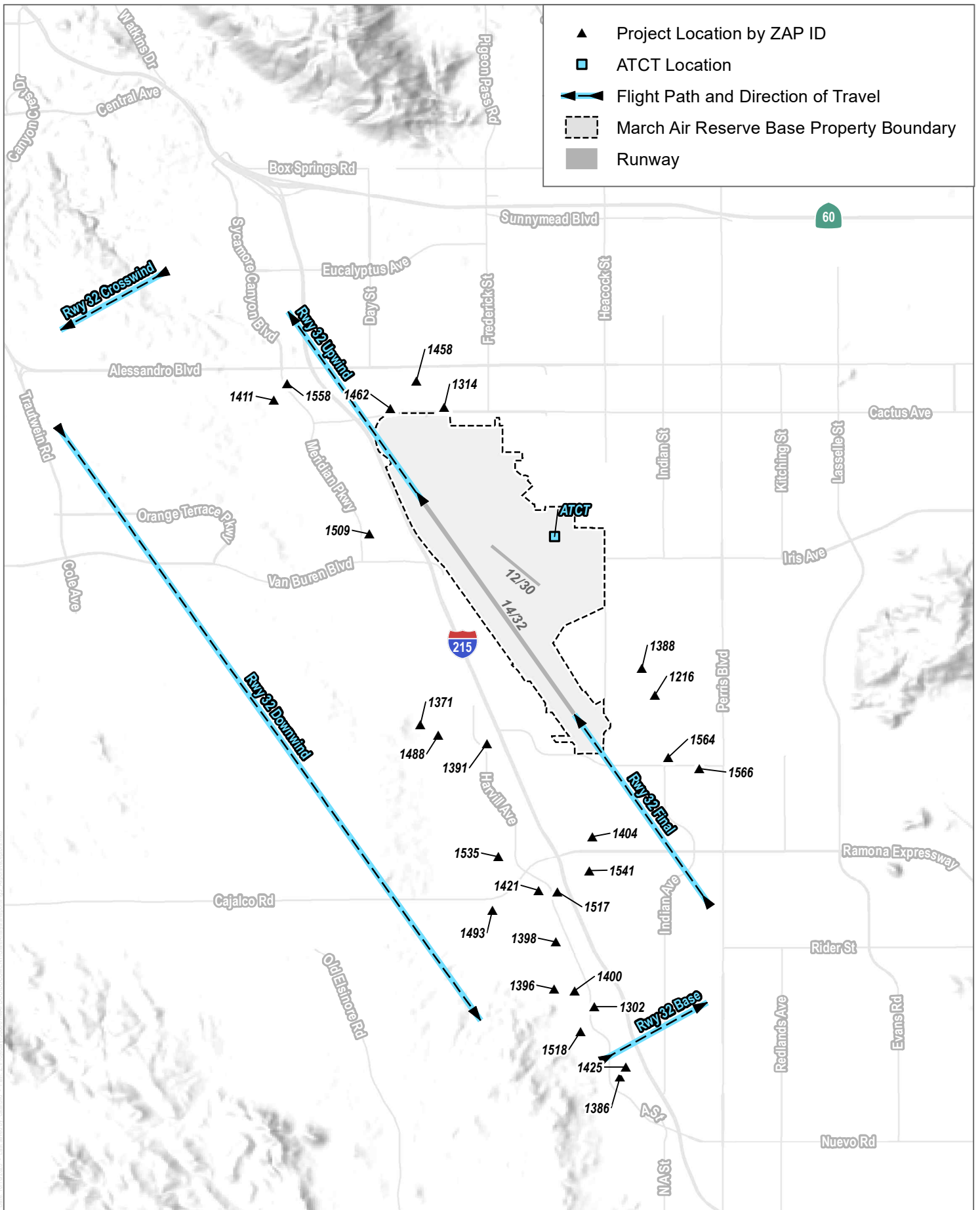
FIGURE 3E

Airport Receptor Locations - Rwy 14 C-17/KC-135 Rectangular Traffic Pattern

DUDEK 0 0.65 1.3 Miles

March Air Reserve Base Compatible Use Study, Cumulative Glare Analysis

INTENTIONALLY LEFT BLANK



SOURCE: Esri and Digital Globe 2023

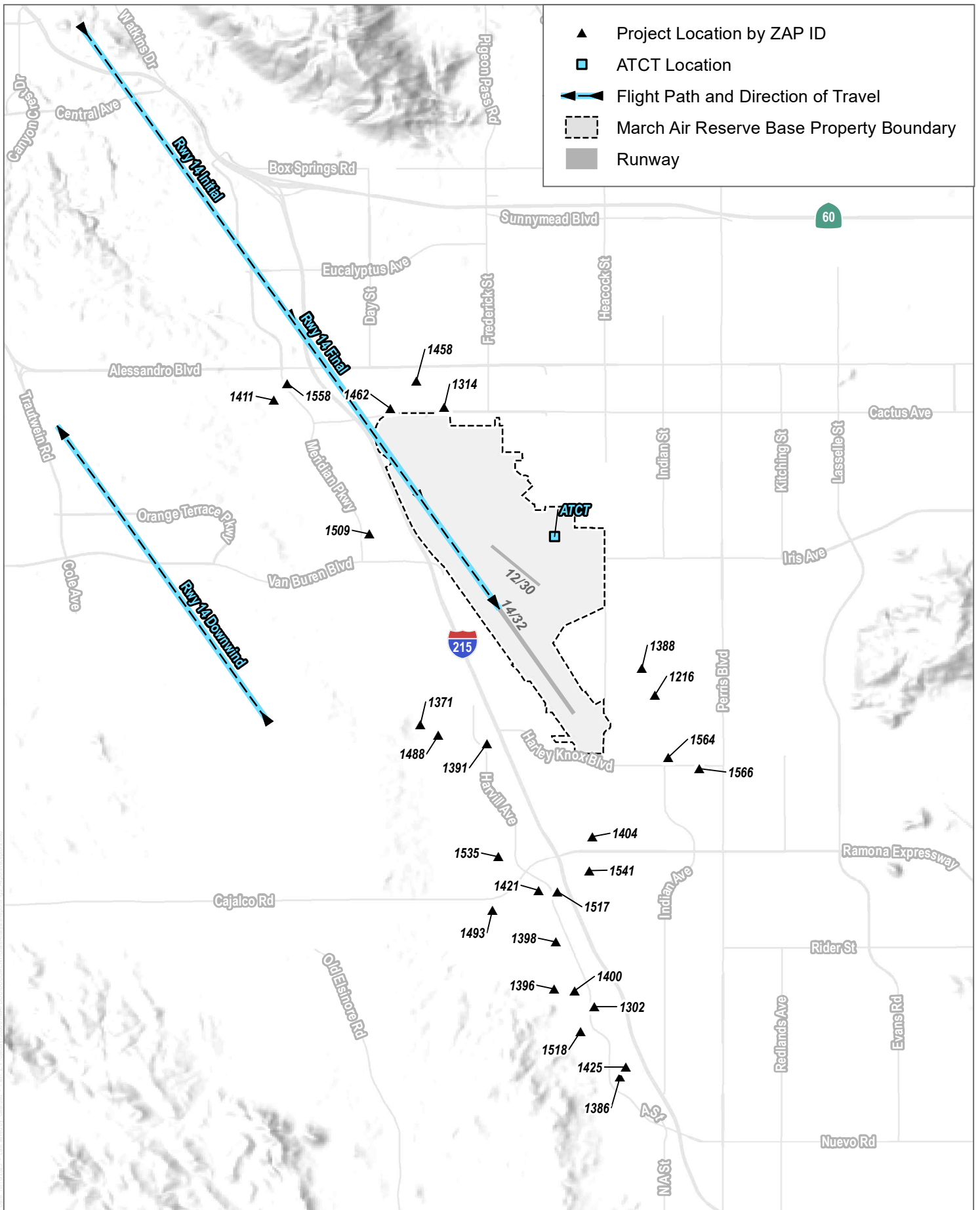
FIGURE 3F

Airport Receptor Locations - Rwy 32 C-17/KC-135 Rectangular Traffic Pattern



March Air Reserve Base Compatible Use Study, Cumulative Glare Analysis

INTENTIONALLY LEFT BLANK



SOURCE: Esri and Digital Globe 2023

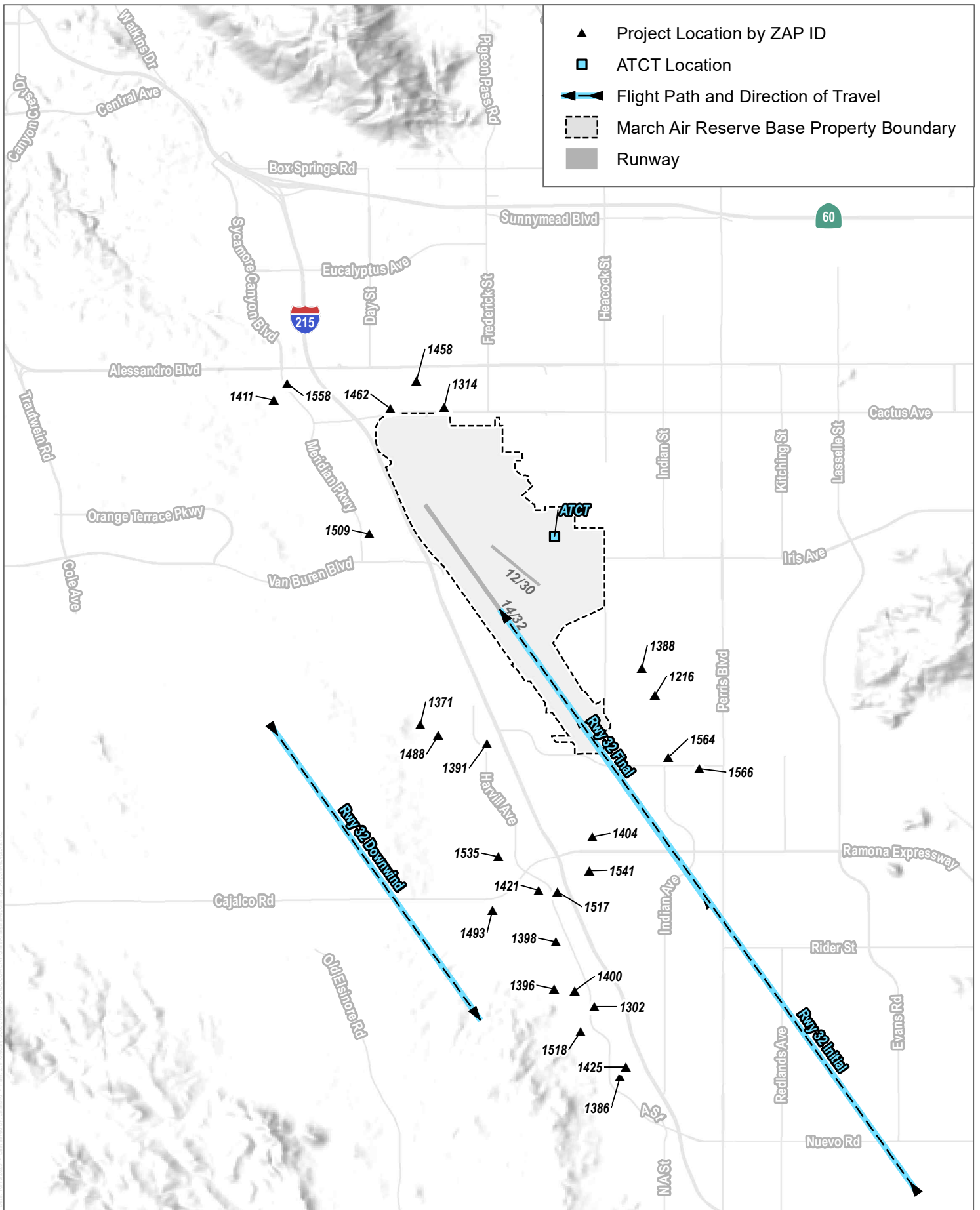
FIGURE 3G

Airport Receptor Locations - Rwy 14 Overhead Traffic Pattern

March Air Reserve Base Compatible Use Study, Cumulative Glare Analysis



INTENTIONALLY LEFT BLANK

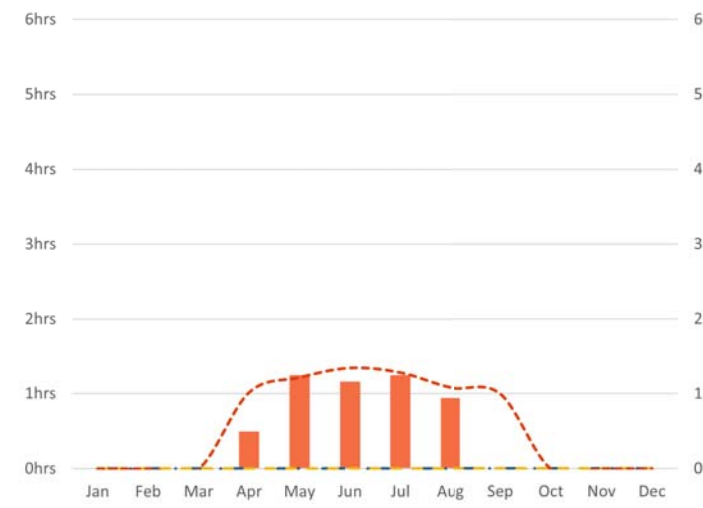


SOURCE: Esri and Digital Globe 2023

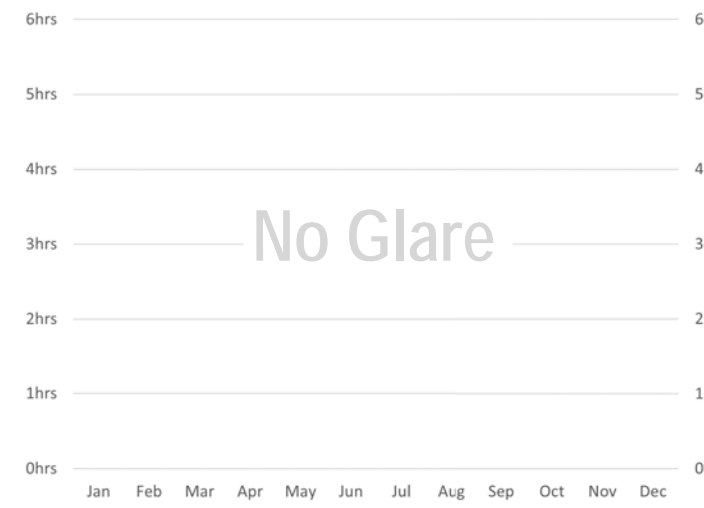
FIGURE 3H
 Airport Receptor Locations - Rwy 32 Overhead Traffic Pattern
 March Air Reserve Base Compatible Use Study, Cumulative Glare Analysis

INTENTIONALLY LEFT BLANK

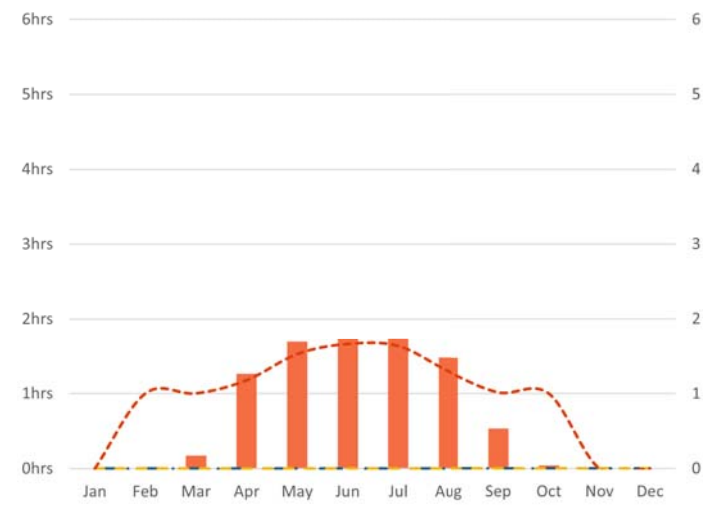
Rwy 12 Base



Rwy 12 Crosswind



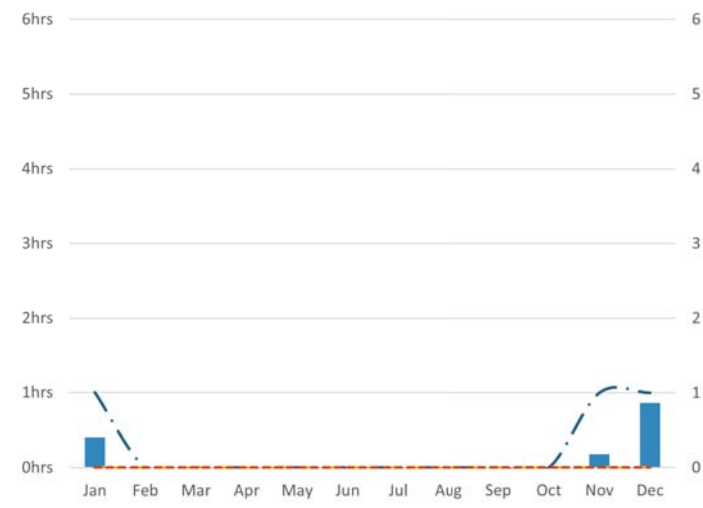
Rwy 12 Downwind



Rwy 12 Final

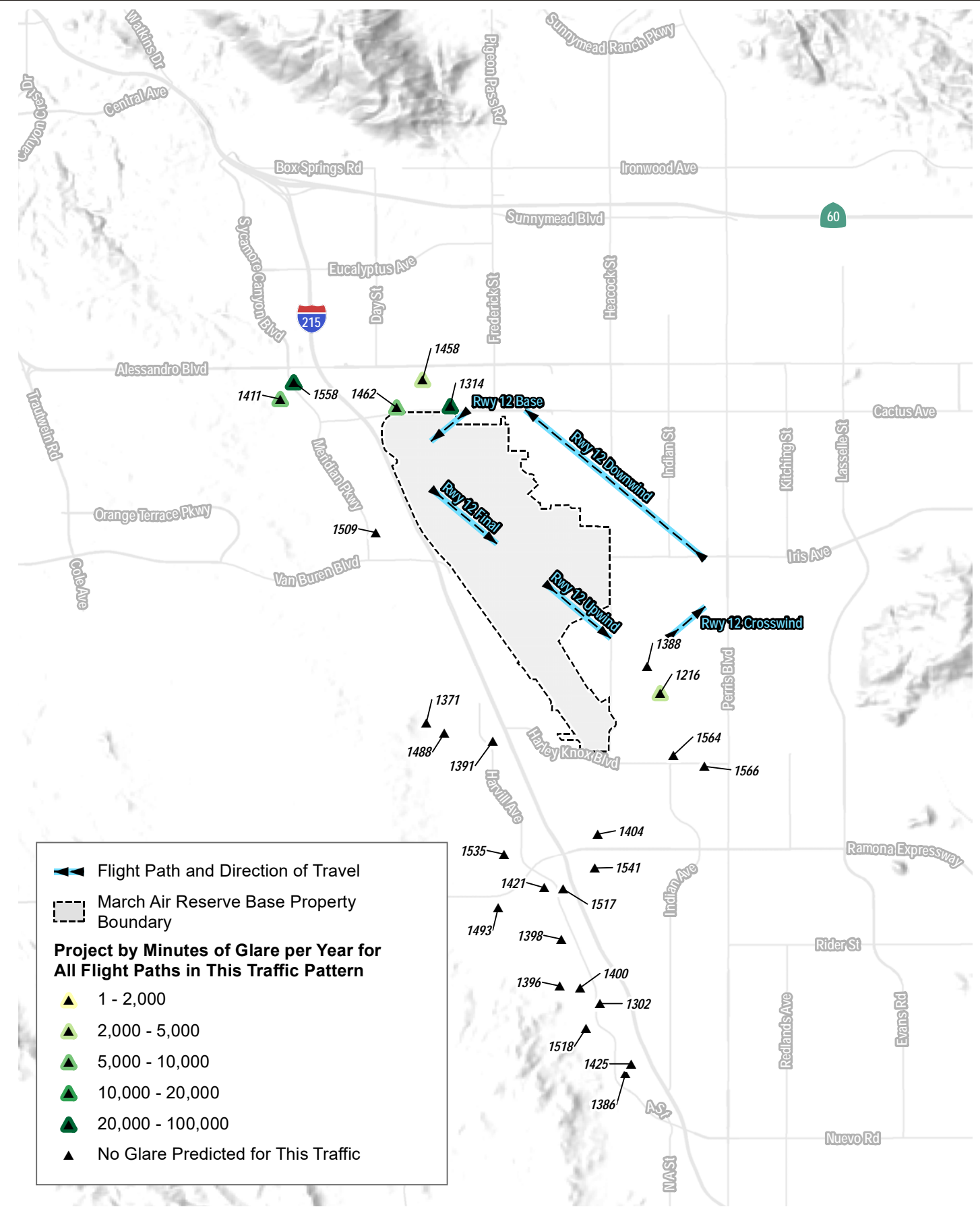


Rwy 12 Upwind



Key

- Evening - Avg. Daily Hours of Glare
- Midday - Avg. Daily Hours of Glare
- Morning - Avg. Daily Hours of Glare
- - - Morning - Avg. Source Count
- - - Midday - Avg. Source Count
- - - Evening - Avg. Source Count

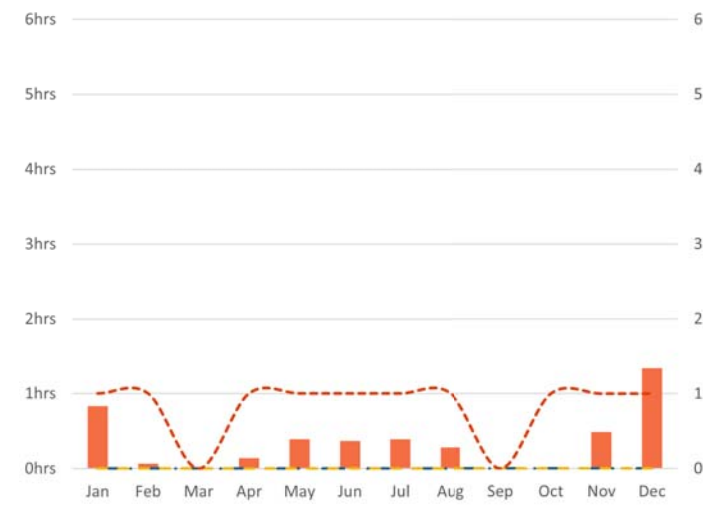


SOURCE: Open Street Map 2019, County of Riverside

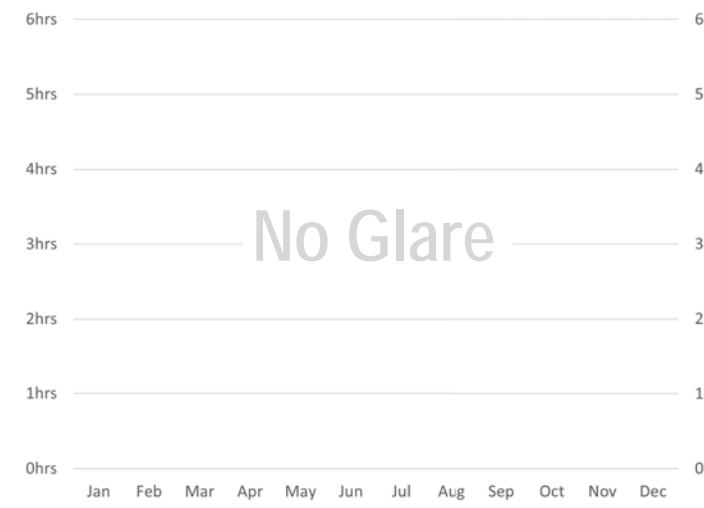
FIGURE 4A
Cumulative Glare Analysis Results – Runway 12 General Aviation Rectangular Traffic Pattern
March Air Reserve Base Compatible Use Study, Cumulative Glare Analysis

INTENTIONALLY LEFT BLANK

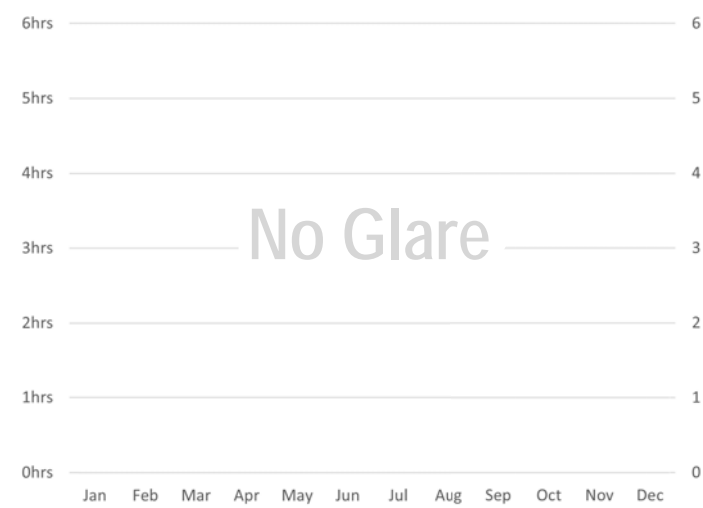
Rwy 30 Base



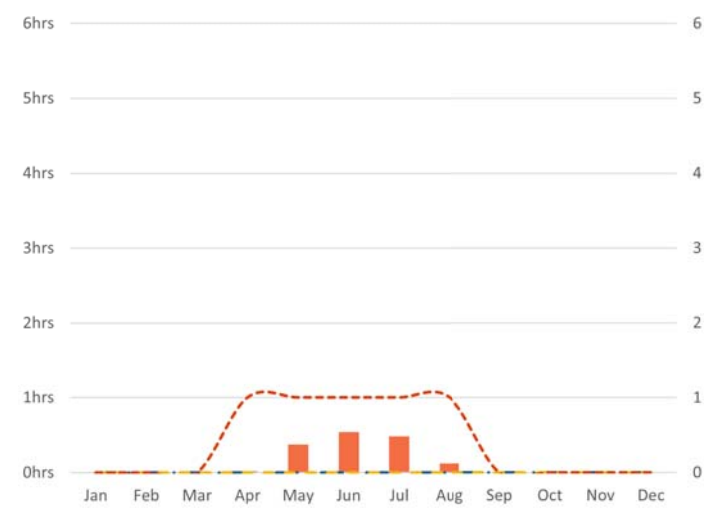
Rwy 30 Crosswind



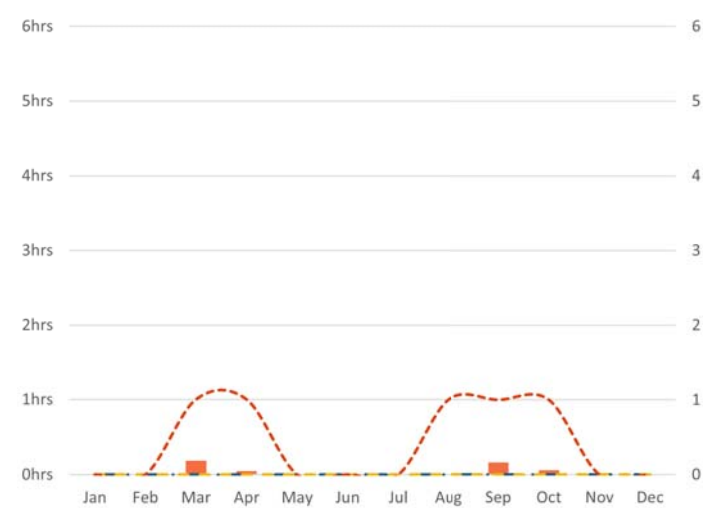
Rwy 30 Downwind



Rwy 30 Final

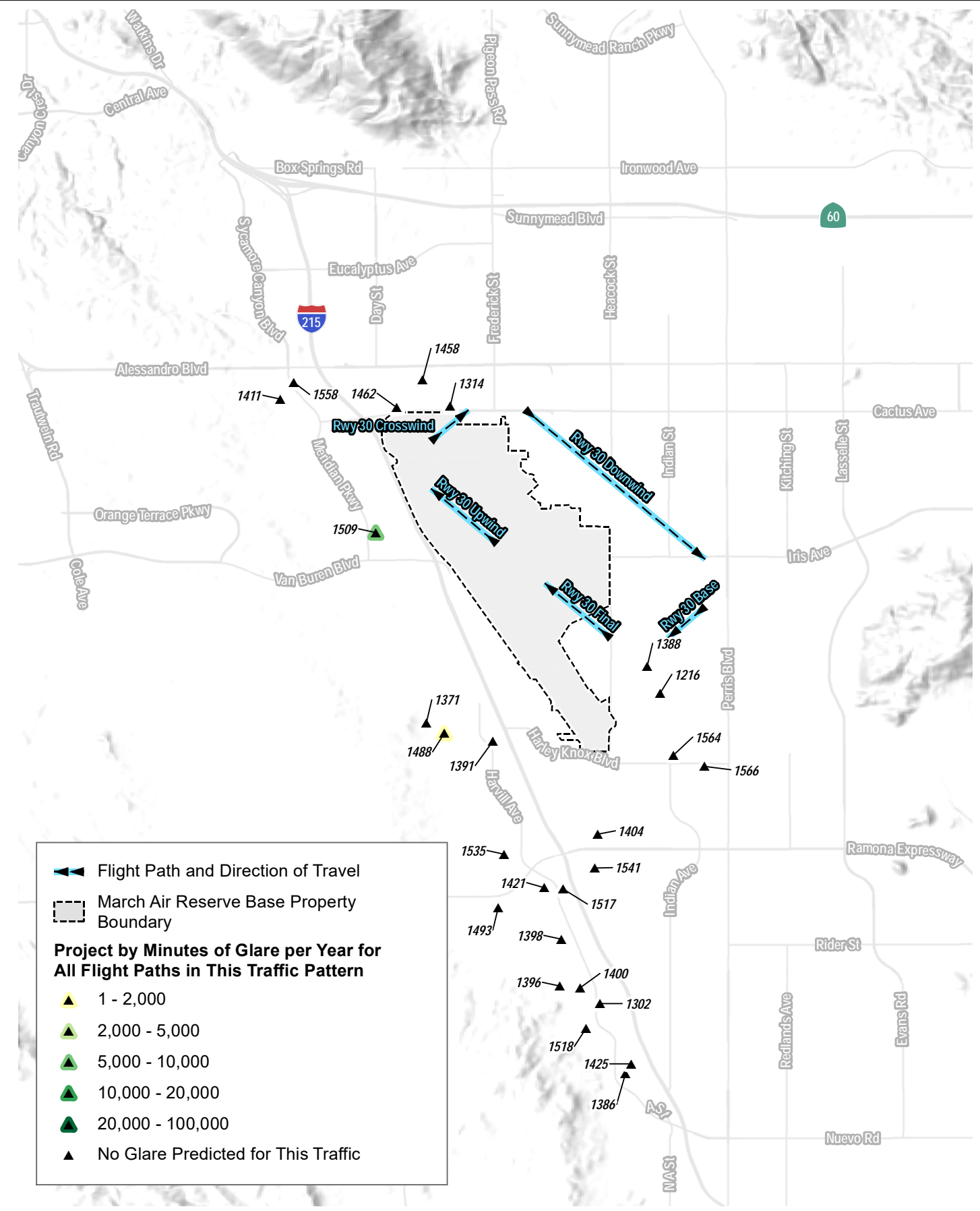


Rwy 30 Upwind



Key

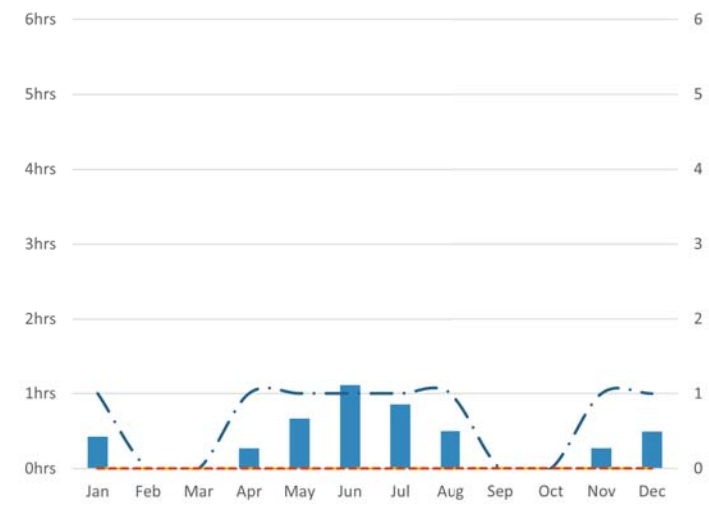
- █ Evening - Avg. Daily Hours of Glare
- █ Midday - Avg. Daily Hours of Glare
- █ Morning - Avg. Daily Hours of Glare
- - - Morning - Avg. Source Count
- - - Midday - Avg. Source Count
- - - Evening - Avg. Source Count



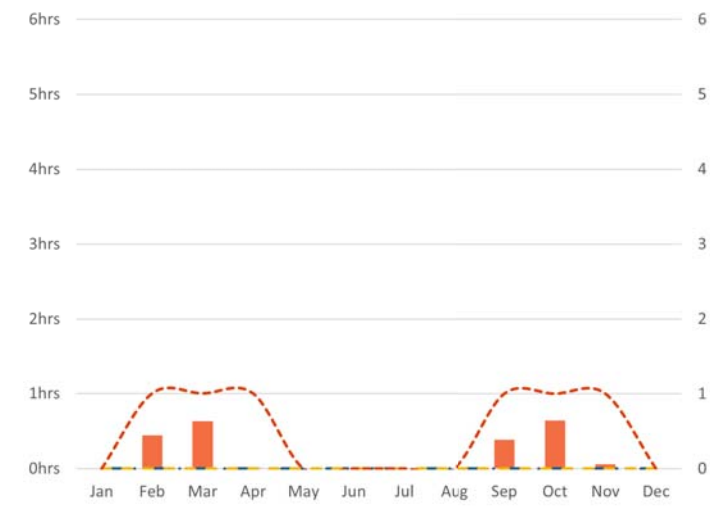
SOURCE: Open Street Map 2019, County of Riverside

INTENTIONALLY LEFT BLANK

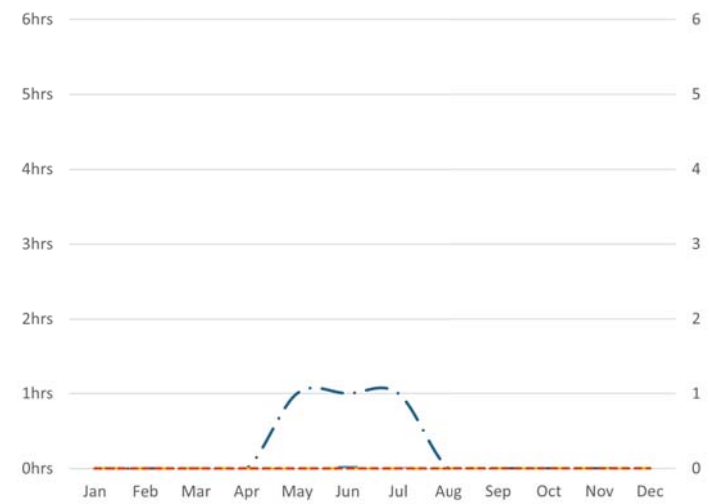
Rwy 14 Base



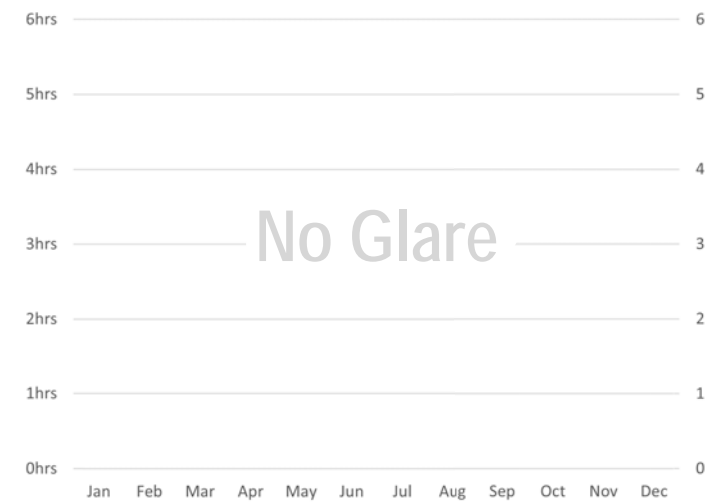
Rwy 14 Crosswind



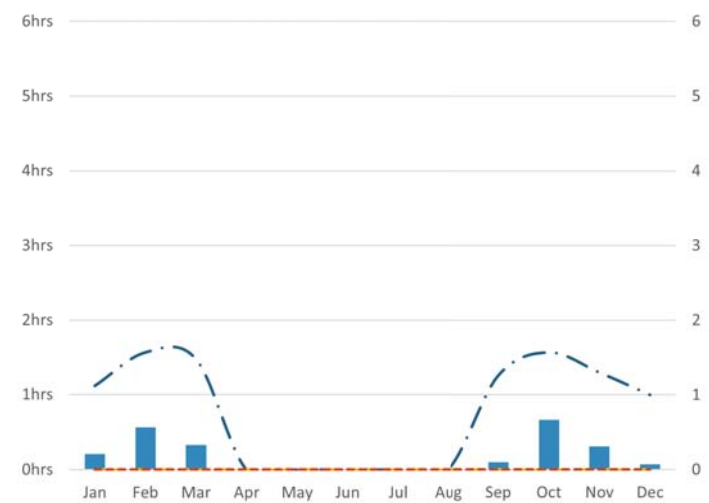
Rwy 14 Downwind



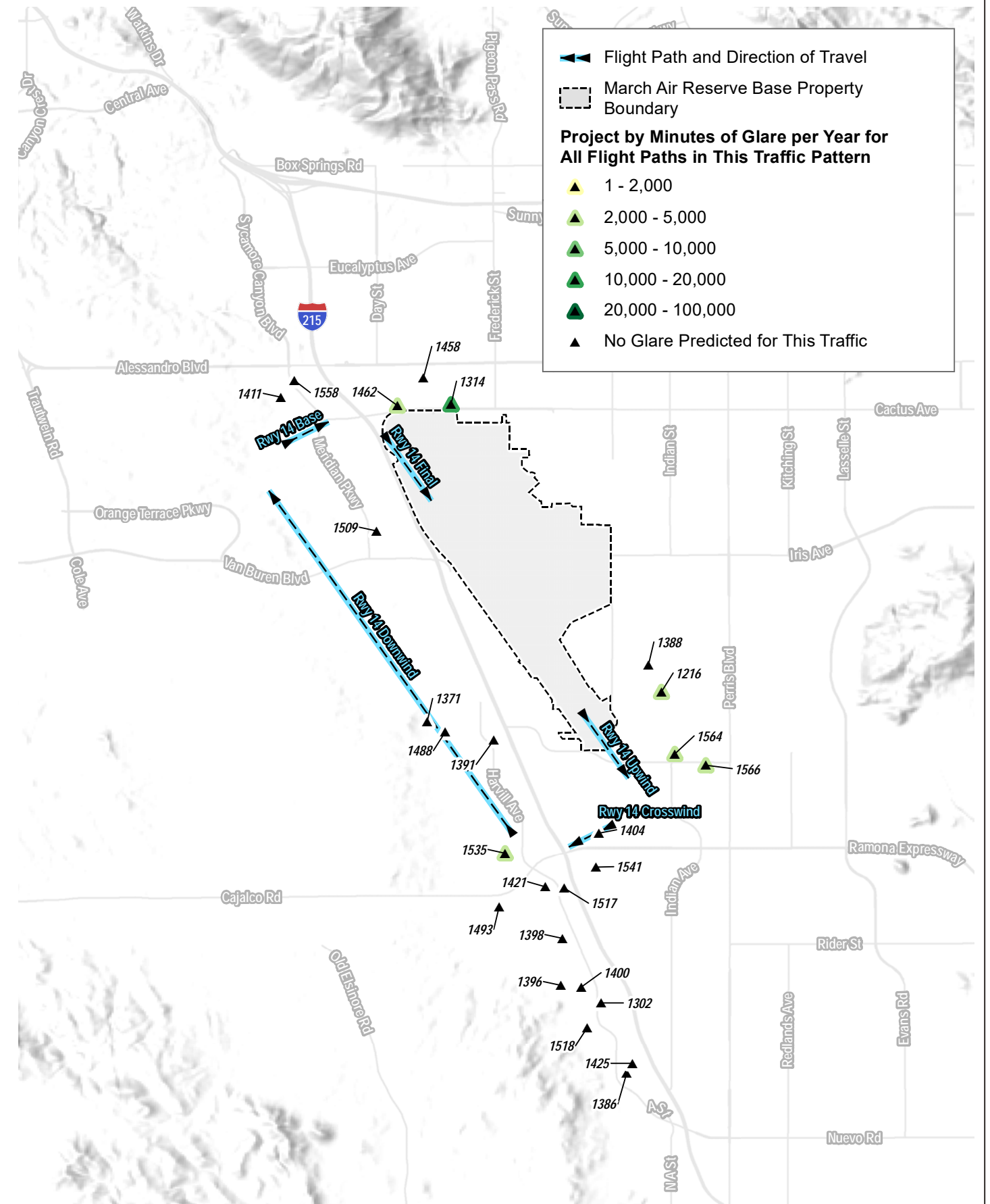
Rwy 14 Final



Rwy 14 Upwind



- Key**
- █ Evening - Avg. Daily Hours of Glare
 - █ Midday - Avg. Daily Hours of Glare
 - █ Morning - Avg. Daily Hours of Glare
 - - - Morning - Avg. Source Count
 - - - Midday - Avg. Source Count
 - - - Evening - Avg. Source Count

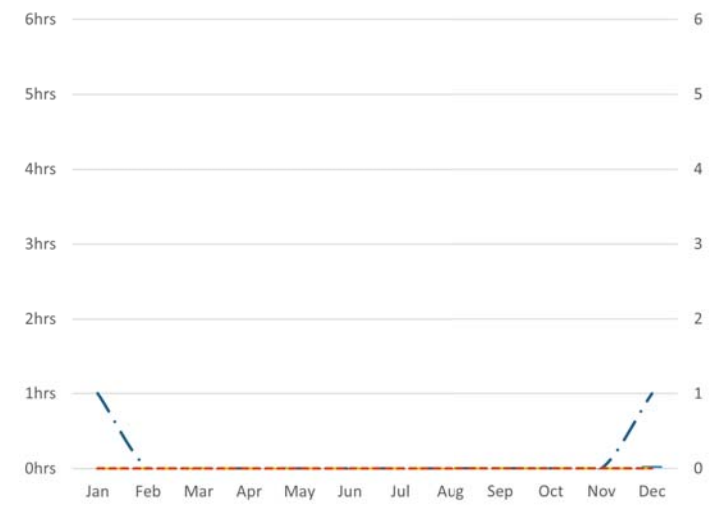


SOURCE: Open Street Map 2019, County of Riverside

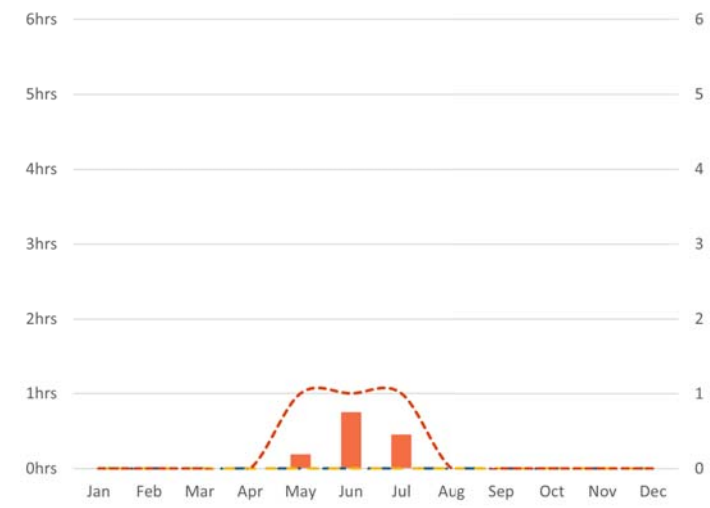
FIGURE 4C
Cumulative Glare Analysis Results - Runway 14 General Aviation Rectangular Traffic Pattern
March Air Reserve Base Compatible Use Study, Cumulative Glare Analysis

INTENTIONALLY LEFT BLANK

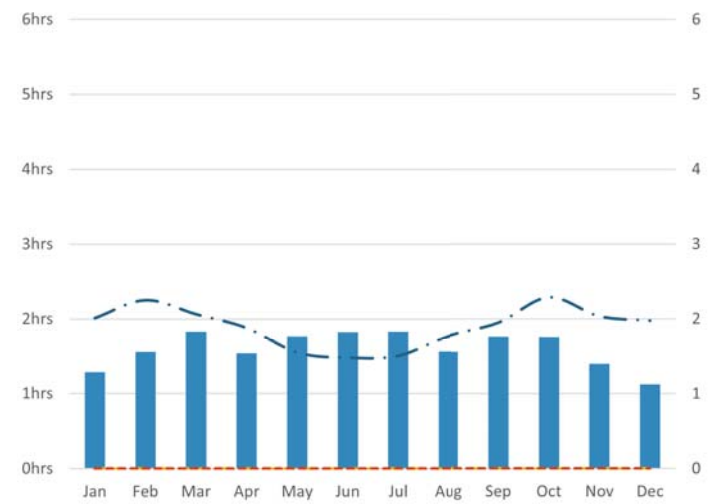
Rwy 32 Base



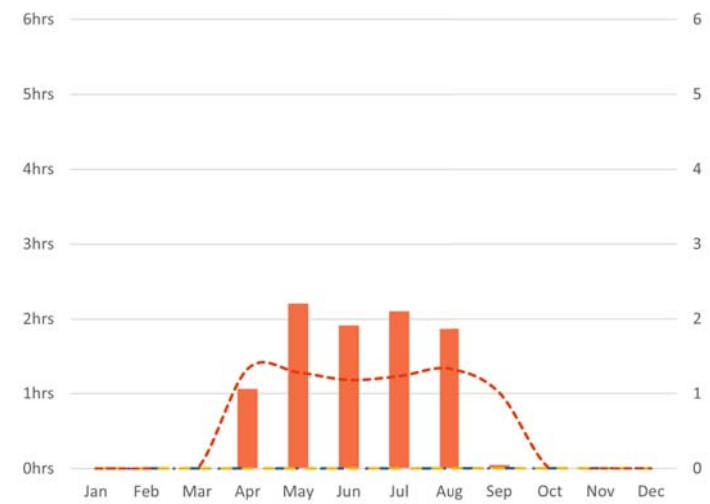
Rwy 32 Crosswind



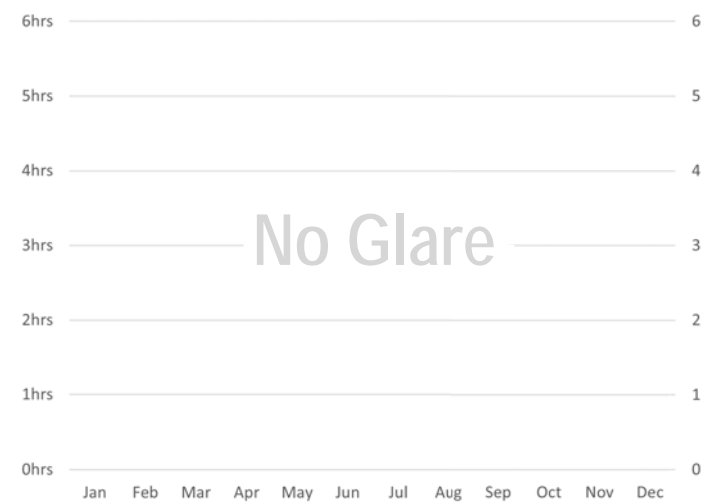
Rwy 32 Downwind



Rwy 32 Final

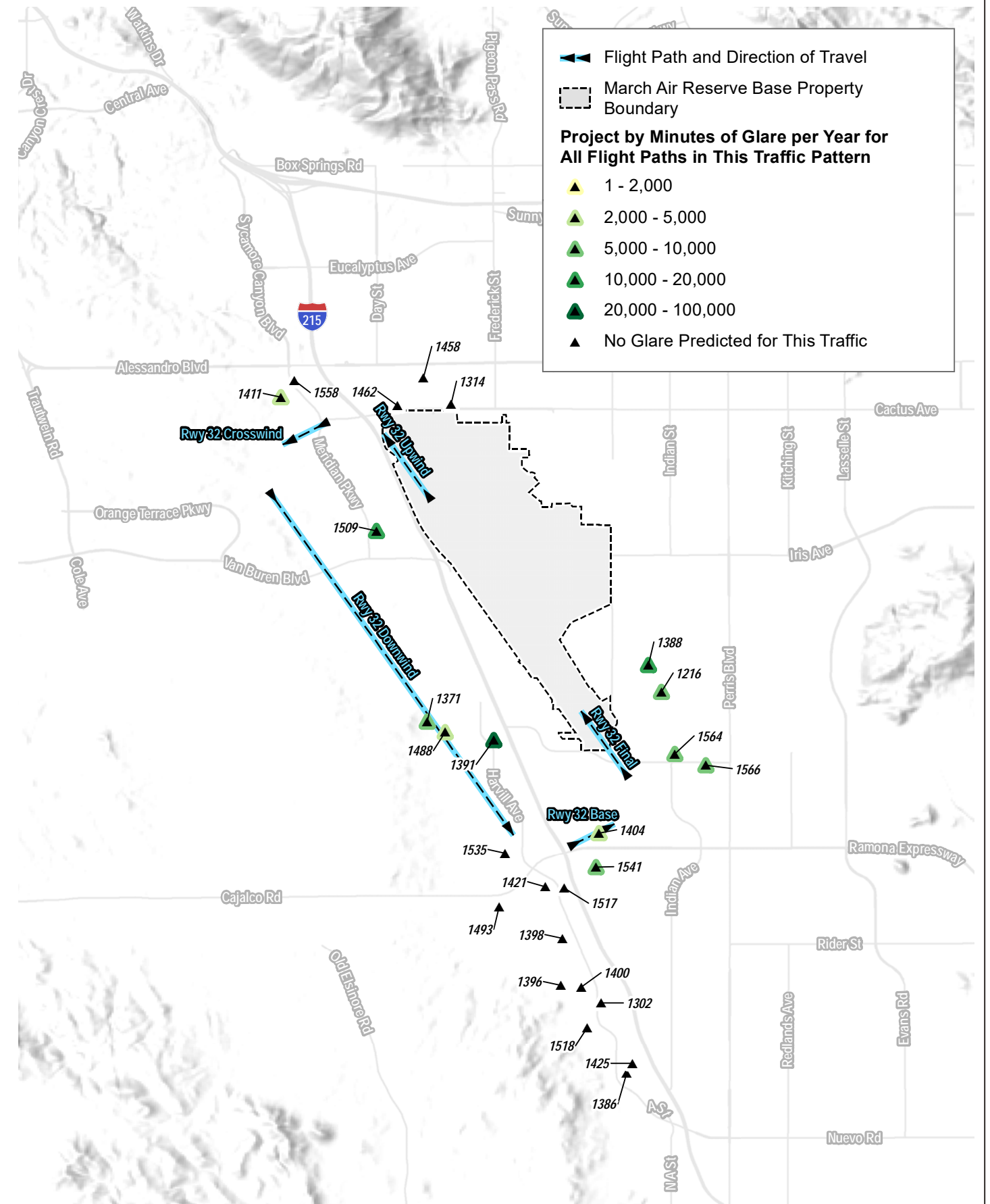


Rwy 32 Upwind



Key

- Evening - Avg. Daily Hours of Glare
- Midday - Avg. Daily Hours of Glare
- Morning - Avg. Daily Hours of Glare
- - - Morning - Avg. Source Count
- - - Midday - Avg. Source Count
- - - Evening - Avg. Source Count

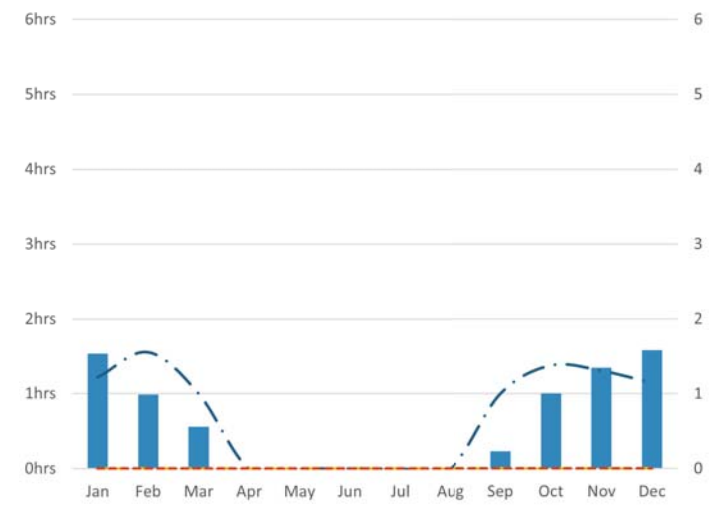


SOURCE: Open Street Map 2019, County of Riverside

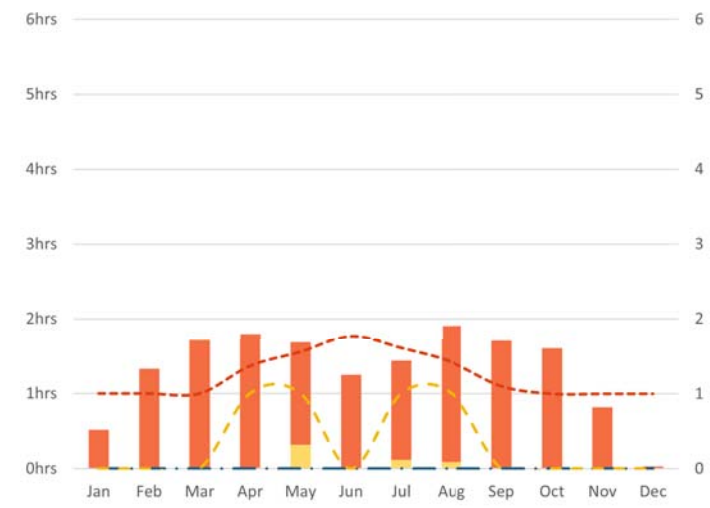
FIGURE 4D
 Cumulative Glare Analysis Results - Runway 32 General Aviation Rectangular Traffic Pattern
 March Air Reserve Base Compatible Use Study, Cumulative Glare Analysis

INTENTIONALLY LEFT BLANK

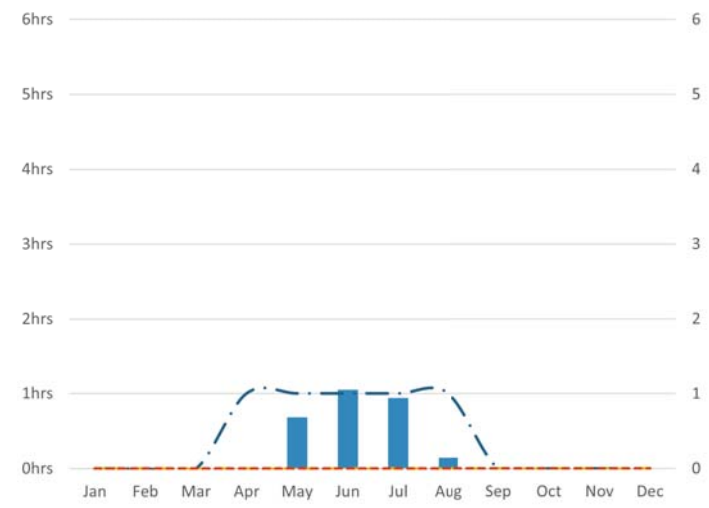
Rwy 14 Base



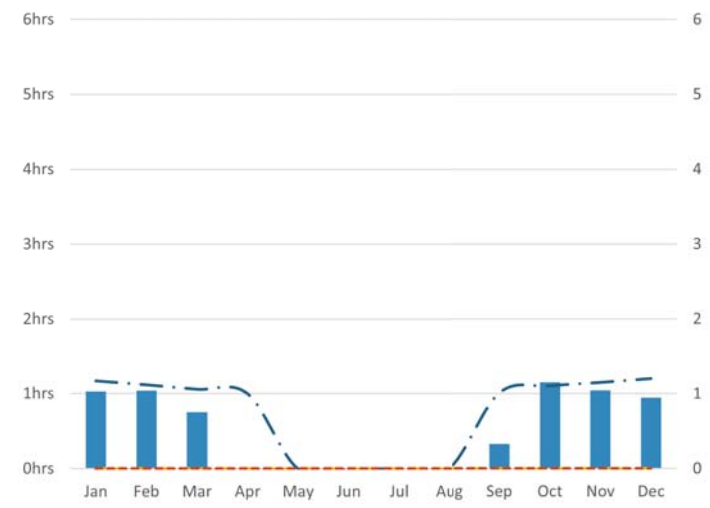
Rwy 14 Crosswind



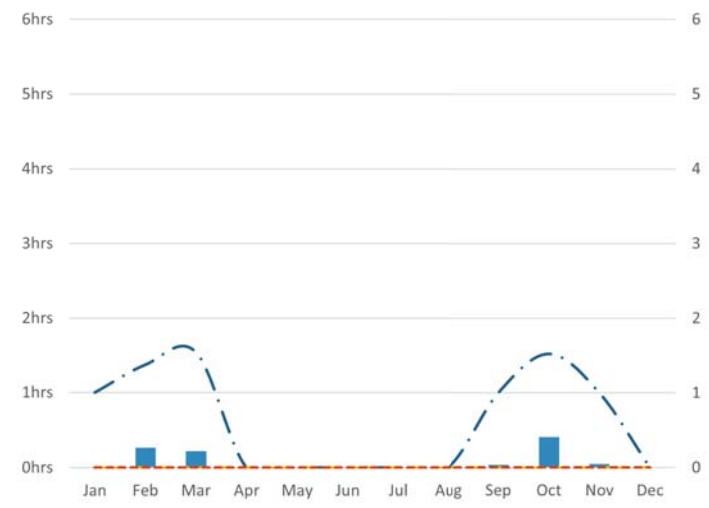
Rwy 14 Downwind



Rwy 14 Final

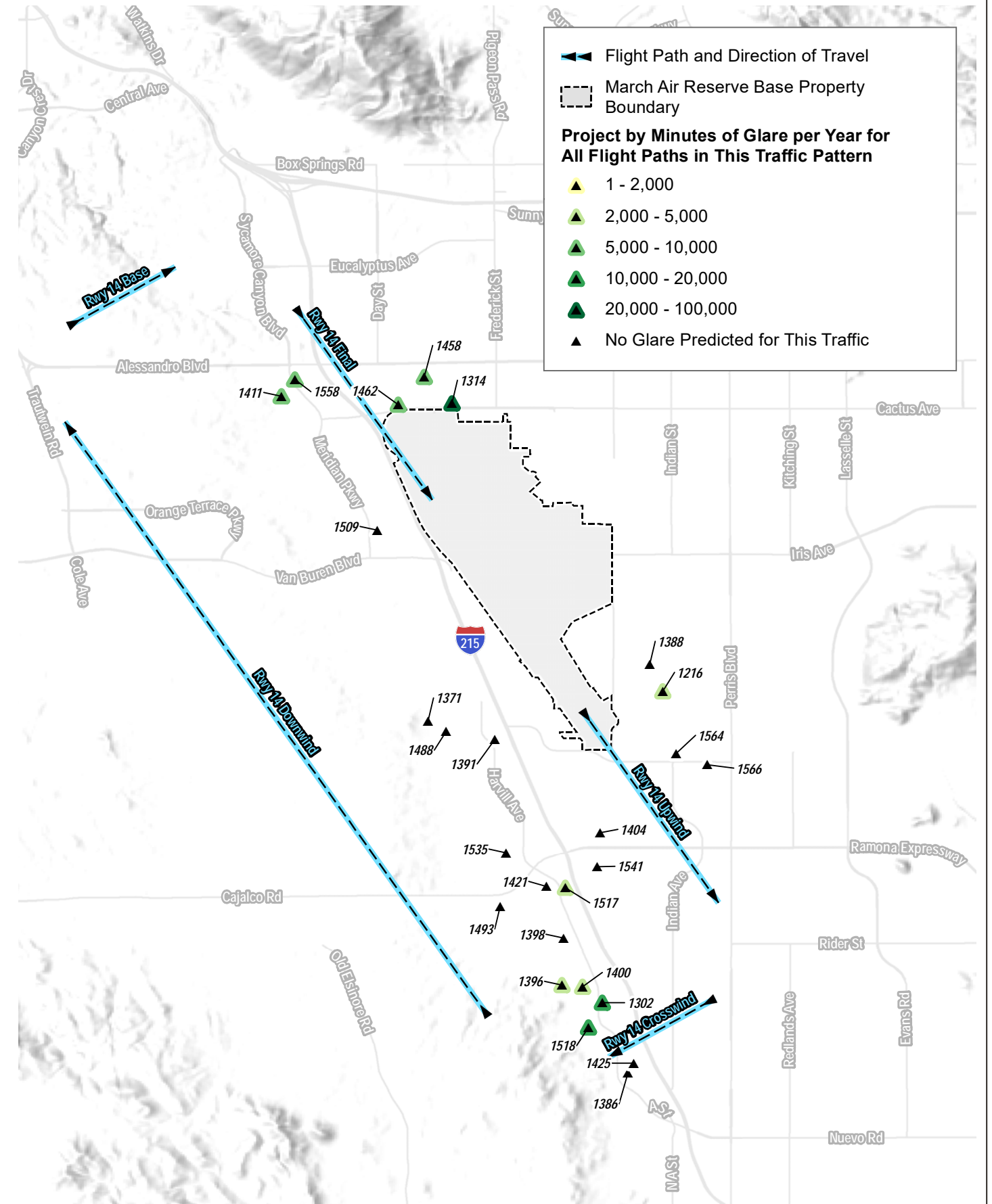


Rwy 14 Upwind



Key

- Evening - Avg. Daily Hours of Glare
- Midday - Avg. Daily Hours of Glare
- Morning - Avg. Daily Hours of Glare
- - - Morning - Avg. Source Count
- - - Midday - Avg. Source Count
- - - Evening - Avg. Source Count

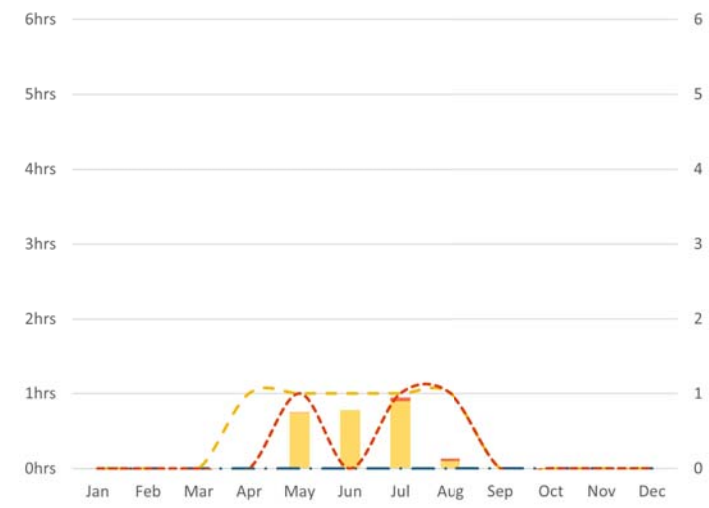


SOURCE: Open Street Map 2019, County of Riverside

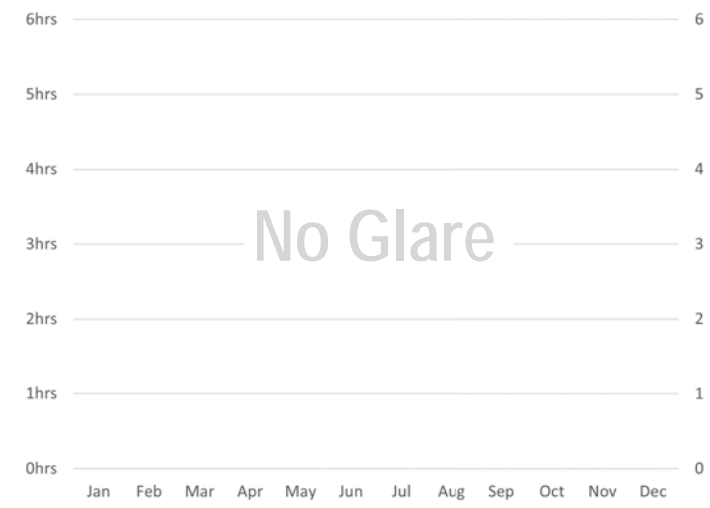
FIGURE 4E
Cumulative Glare Analysis Results - Runway 14 C-17/KC-135 Rectangular Traffic Pattern
March Air Reserve Base Compatible Use Study, Cumulative Glare Analysis

INTENTIONALLY LEFT BLANK

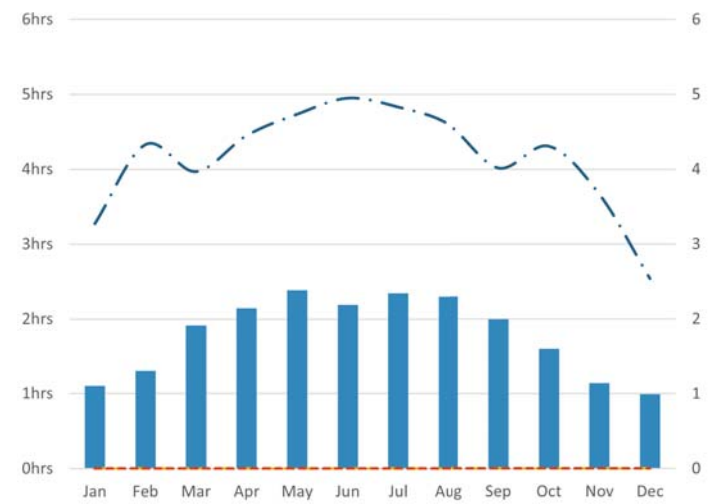
Rwy 32 Base



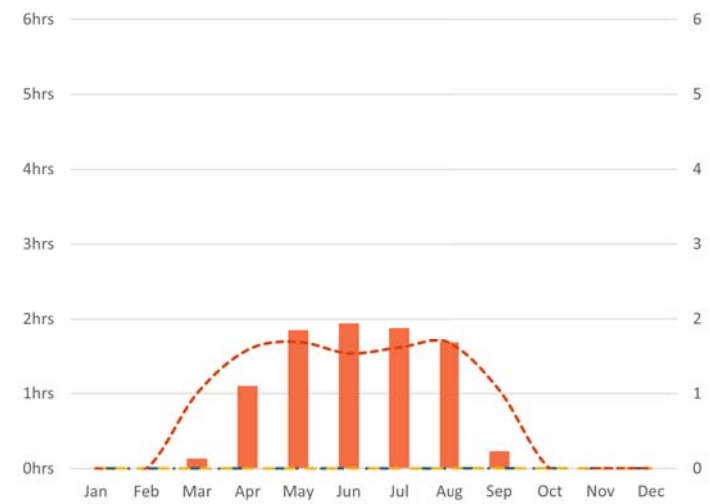
Rwy 32 Crosswind



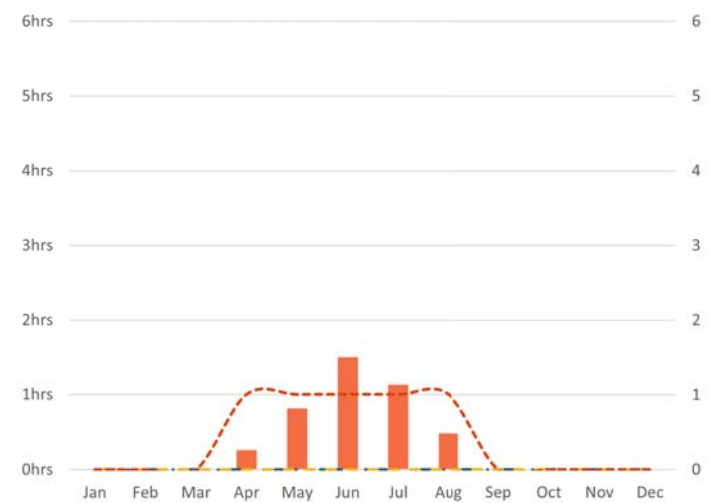
Rwy 32 Downwind



Rwy 32 Final

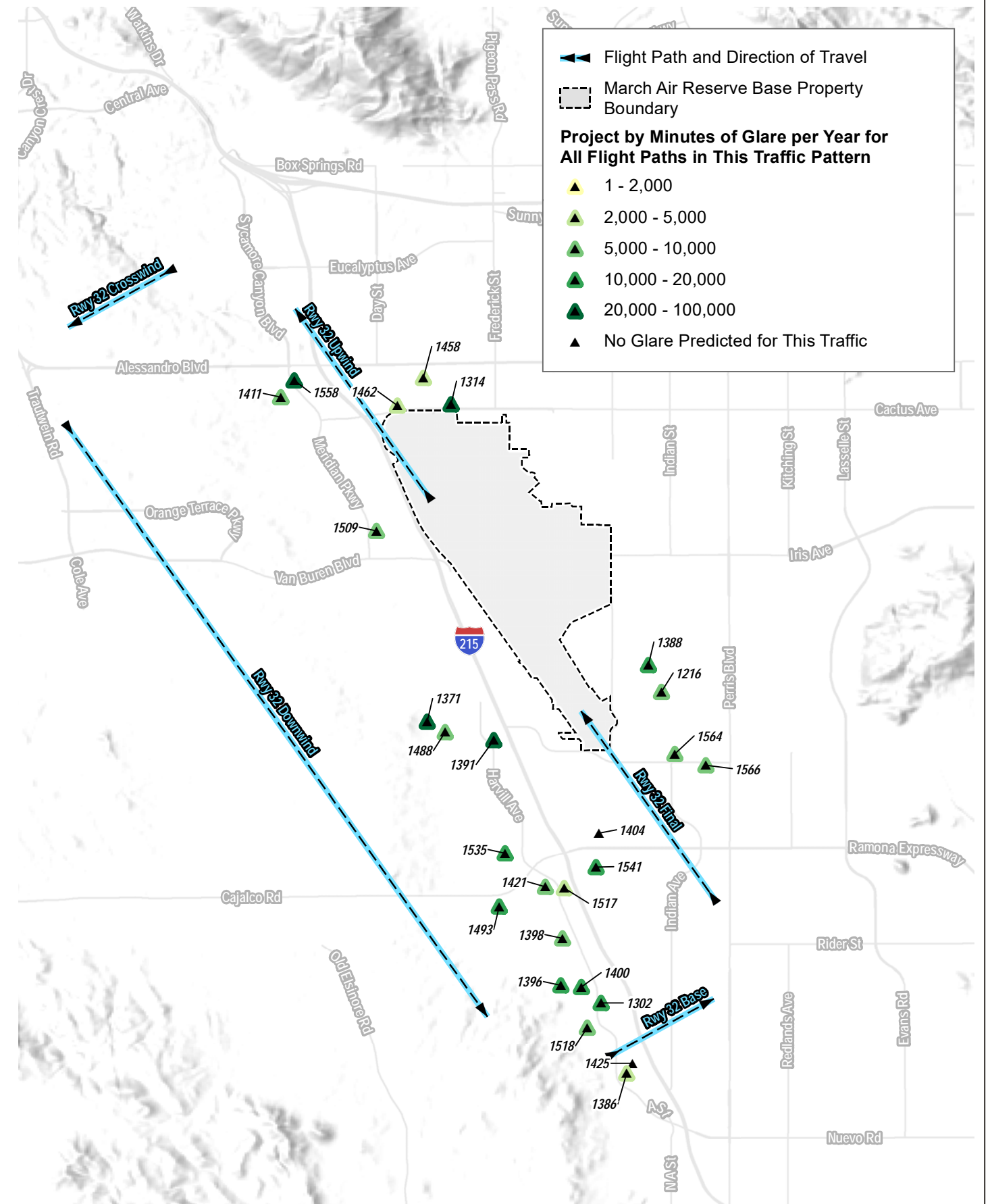


Rwy 32 Upwind



Key

- Evening - Avg. Daily Hours of Glare
- Midday - Avg. Daily Hours of Glare
- Morning - Avg. Daily Hours of Glare
- Morning - Avg. Source Count
- Midday - Avg. Source Count
- Evening - Avg. Source Count

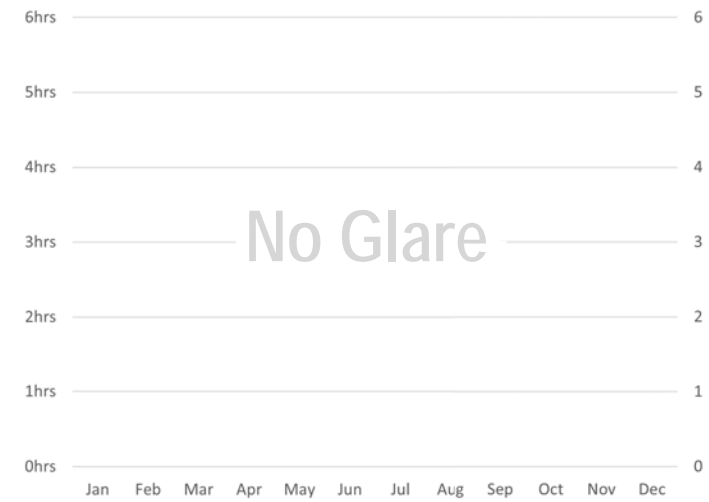


SOURCE: Open Street Map 2019, County of Riverside

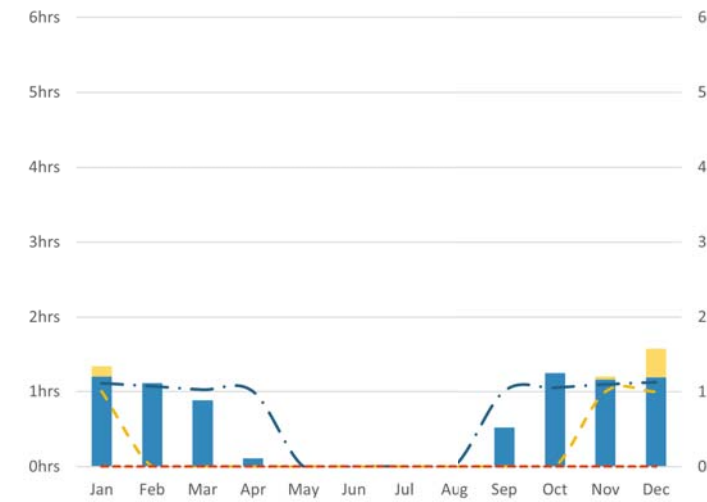
FIGURE 4F
Cumulative Glare analysis Results - Runway 32 C-17/KC-135 Rectangular Traffic Pattern
March Air Reserve Base Compatible Use Study, Cumulative Glare Analysis

INTENTIONALLY LEFT BLANK

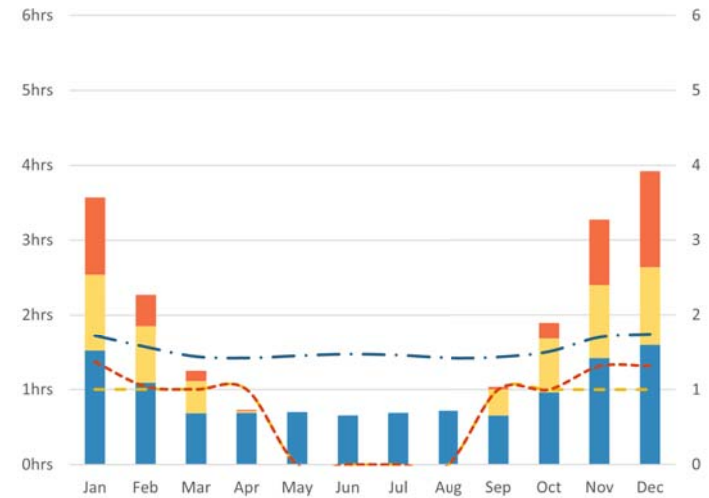
Rwy 14 Downwind



Rwy 14 Final

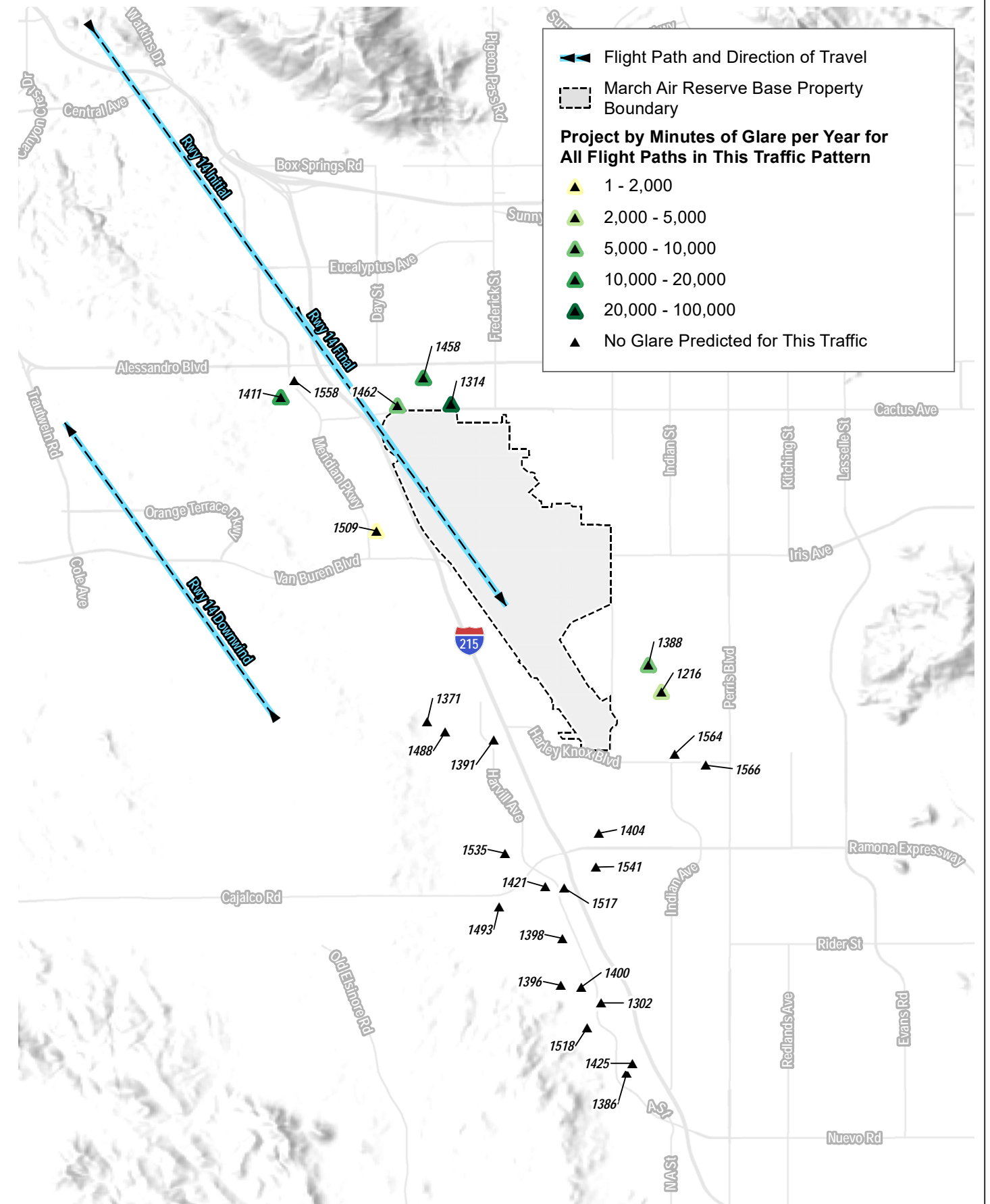


Rwy 14 Initial



Key

- Evening - Avg. Daily Hours of Glare
- Midday - Avg. Daily Hours of Glare
- Morning - Avg. Daily Hours of Glare
- - - Morning - Avg. Source Count
- - - Midday - Avg. Source Count
- - - Evening - Avg. Source Count



SOURCE: Open Street Map 2019, County of Riverside

FIGURE 4G

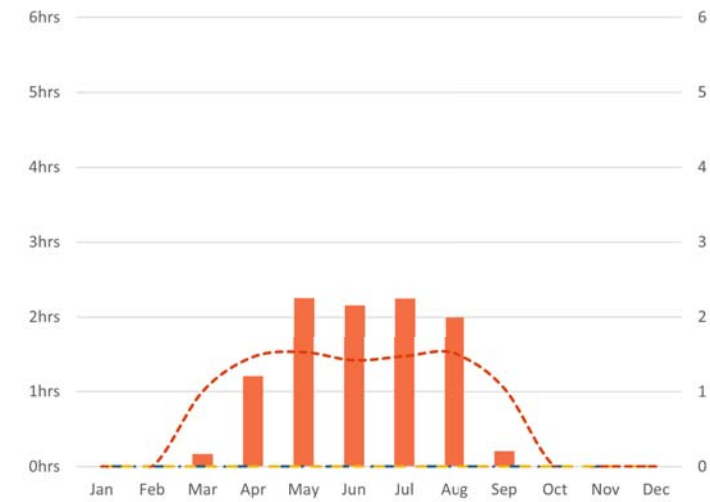
Cumulative Glare Analysis Results – Runway 14 Overhead Traffic Pattern
March Air Reserve Base Compatible Use Study, Cumulative Glare Analysis

INTENTIONALLY LEFT BLANK

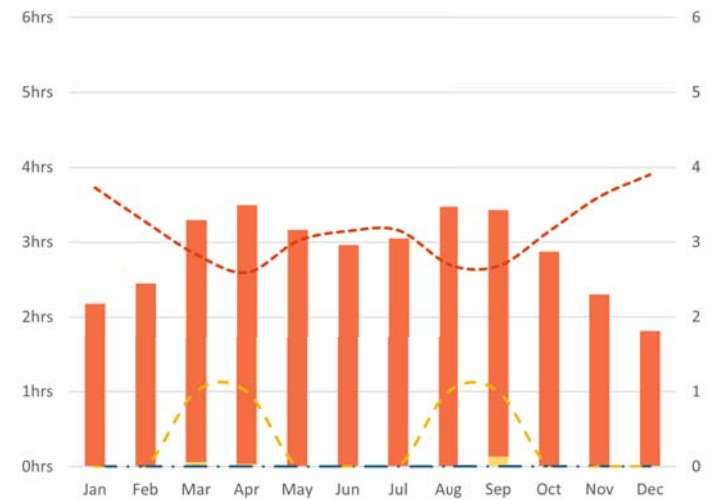
Rwy 32 Downwind



Rwy 32 Final

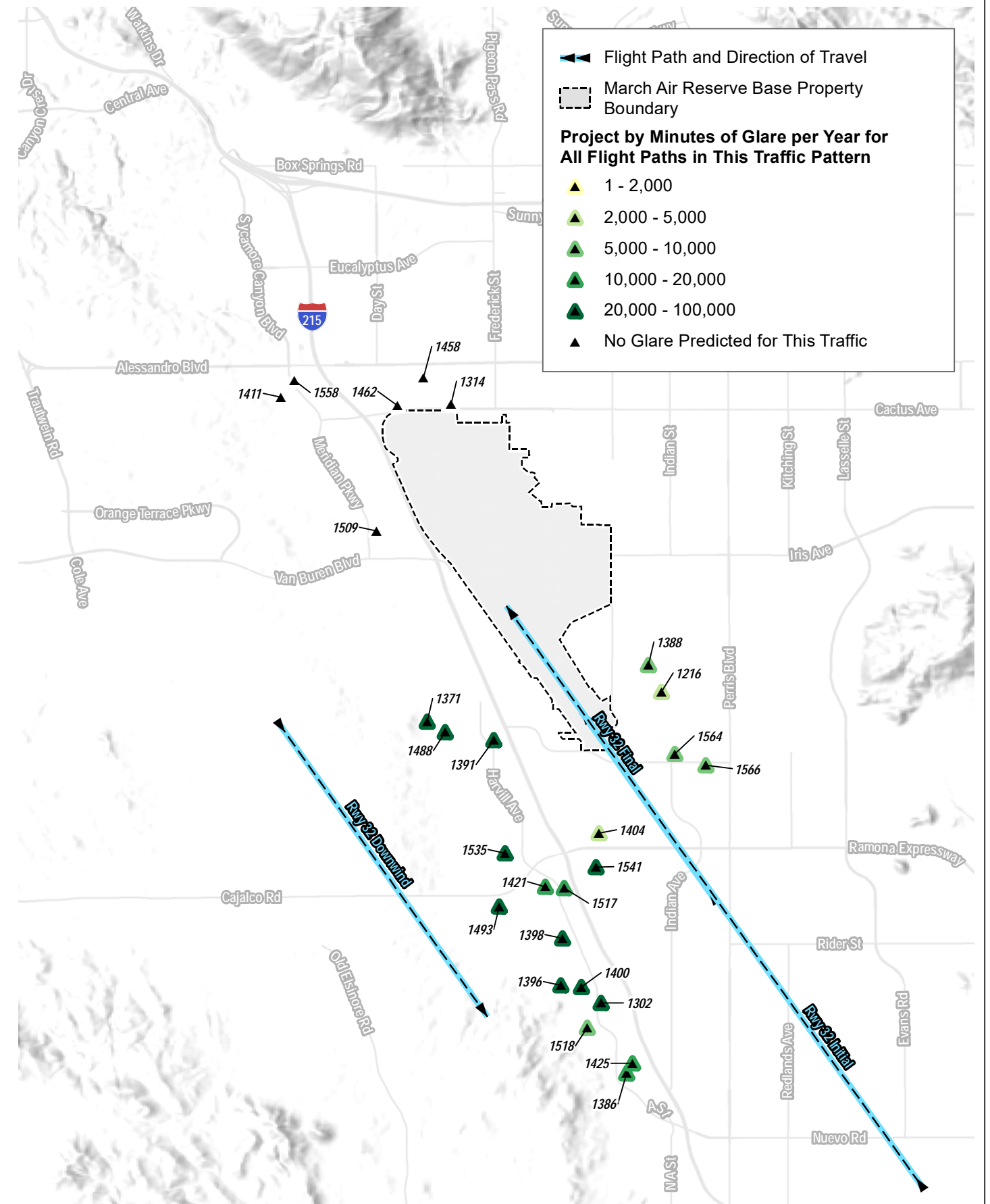


Rwy 32 Initial



Key

- Evening - Avg. Daily Hours of Glare
- Midday - Avg. Daily Hours of Glare
- Morning - Avg. Daily Hours of Glare
- - - Morning - Avg. Source Count
- - - Midday - Avg. Source Count
- - - Evening - Avg. Source Count



SOURCE: Open Street Map 2019, County of Riverside

INTENTIONALLY LEFT BLANK

INTENTIONALLY LEFT BLANK

Appendix A

Detailed Modeling Results